Geological Society of America Bulletin

The stratigraphic evolution of the El Paso basin, southern California: Implications for the Miocene development of the Garlock fault and uplift of the Sierra Nevada

DANA P. LOOMIS and DOUGLAS W. BURBANK

Email alerting services	click www.gsapubs.org/cgi/alerts to receive free e-mail alerts when new articles cite this article
Subscribe	click www.gsapubs.org/subscriptions/ to subscribe to Geological Society of America Bulletin
Permission request	click http://www.geosociety.org/pubs/copyrt.htm#gsa to contact GSA

Notes

The stratigraphic evolution of the El Paso basin, southern California: Implications for the Miocene development of the Garlock fault and uplift of the Sierra Nevada

DANA P. LOOMIS   *Department of Geology, University of North Carolina, Chapel Hill, North Carolina 27514*
DOUGLAS W. BURBANK   *Department of Geological Sciences, University of Southern California, Los Angeles, California 90089-0740*

ABSTRACT

The Ricardo Group is a 1,700-m-thick sequence of Miocene volcanic rocks and continental sedimentary rocks deposited between ~19 and 7 Ma in the El Paso basin, near the junction of the Garlock fault and the Sierra Nevada frontal fault in southern California. The combination of stratigraphic and structural data from the Ricardo Group with chronologic and rotational histories derived from magnetostratigraphic and radiometric studies provides some new constraints for the morphotectonic emergence of the Sierra Nevada, the initiation of strike-slip movement on the Garlock fault, and related east-west extension in the southern Basin and Range region. The Miocene sequence documents (1) volcanism and north-south tension without net extension at 18–15 Ma (2) relative uplift about 15–13.5 Ma, (3) the beginning of sinistral slip on the Garlock fault and east-west extension in the southwestern Basin and Range region about 10–9 Ma, and (4) emergence of the Sierra Nevada as a source area and topographic high by 8 Ma.

Stratigraphic evidence from the Ricardo Group does not indicate significant Miocene dip-slip movement along the large-scale, down-to-the-north fault that has been previously hypothesized to have preceded the present Garlock fault in the same location during the early Tertiary. The evolution of this sequence, however, can be explained by tectonic models which propose a time-space linkage between basin evolution, east-west extension in southern California, and the Mendocino triple-junction system.

INTRODUCTION

Major structural boundaries frequently delimit tectonic provinces exhibiting contrasting histories and deformational styles. An understanding of the geological development of such boundary zones can illuminate the timing and nature of events that caused the present juxtapositions of contrasting terranes. In southern California, the Garlock fault and, to a lesser extent, the Sierra Nevada frontal fault represent this type of delimiting tectonic boundary. The late Cenozoic geology of the Basin and Range region north and east of these faults has been largely shaped by east-west extension, whereas the Mojave province to the south has been relatively unaffected by it. The El Paso basin is virtually astride the line dividing these geologic regions, and the evolution of the basin and its nearly 2 km of late Cenozoic sedimentary and volcanic fill have been directly influenced by the development of the Garlock fault and the uplift of the Sierra Nevada.

This paper presents the results of stratigraphic, chronologic, and tectonic investigations of the Miocene Ricardo Group in the El Paso basin. Sedimentary and magnetostratigraphic data provide evidence for the onset of east-west extension north of the Garlock fault about 10 Ma and for the emergence of the Sierra Nevada as a topographic upland about 8 Ma. In addition to these age constraints for the Garlock fault and Sierra Nevada, this analysis also provides an opportunity to test some plate-tectonic models for the late Cenozoic sedimentary and tectonic evolution of southern California. Sedimentary evidence from the El Paso basin is largely consistent with proposals that basin growth and sedimentation (Glazner and Loomis, 1984) and basin-and-range extension (Ingersoll, 1982; Glazner and Bartley, 1984) in southern California are temporally associated with the reconstructed latitude of the Mendocino triple-junction system and can be explained by interactions between the Mendocino fracture zone and the North American plate.

TECTONIC SETTING OF THE EL PASO BASIN

The El Paso basin is located on the north side of the El Paso Mountains 5–6 km north of the Garlock fault in Kern County, California (Fig. 1). Its western boundary is the Sierra Nevada and the Sierra Nevada frontal fault system. Tilted and faulted Tertiary rocks of the basin are exposed in an east-northeast–trending belt about 33 km by 7 km, and they are covered on the north and east by Quaternary alluvial deposits.

The El Paso Mountains are bounded on their southern margin by the El Paso fault (Fig. 1). This fault appears to be a splay of the Garlock fault, but unlike the Garlock fault, it appears to be a dip-slip fault with little or no sinistral offset. The Garlock fault separates the mountains of the Tehachapi, Sierra Nevada, and Basin and Range provinces on the north from the lower-relief Mojave province to the south (Fig. 1). It is a major left-slip intracontinental transform fault which bounds the east-west extension of the Basin and Range and allows the Mojave block to remain relatively unextended (Hamilton and Myers, 1966; Davis and Burchfiel, 1973). The total lateral displacement on the fault is estimated to be at least 64 km (Smith, 1962; Smith and Ketner, 1970; Davis and Burchfiel, 1973). Abundant geomorphic evidence indicates Quaternary left slip on the Garlock fault near the El Paso Mountains (Dibblee, 1952; Clark, 1973; Carter, 1980; La Violette and others, 1980), but the age of the beginning of left slip in this area has not previously been constrained to an interval more precise than some time during the Tertiary. It has often been postulated that the present strike-slip Garlock fault was preceded by a large, high-angle dip-slip (Hewett, 1954; Smith, 1962) or strike-slip (Nilsen and Clarke, 1975) fault as early as Paleocene time. The evidence for both

Figure 1. Generalized geologic map of the El Paso basin and surrounding area. Tertiary sediments of El Paso basin include Tru, Ricardo Group undivided; Tmd, Dove Spring Formation, members 1–5; Tmc, Cudahy Camp Formation; Tpg, Goler Formation. El Paso Mountains basement complex: Mzg, Mesozoic granitoid complex; Mzm, Mesquite schist; Pzm, Paleozoic metamorphic rocks, including the Garlock Formation.
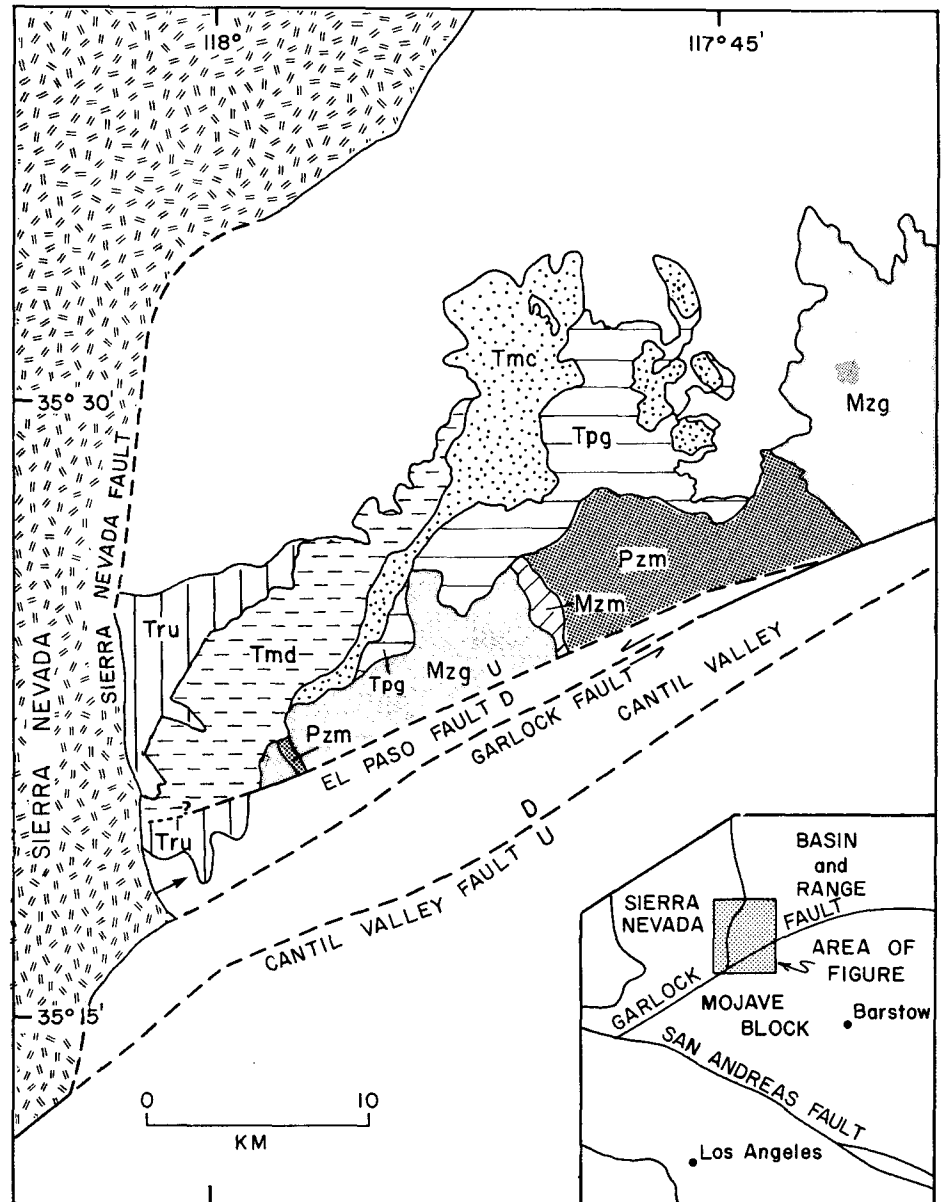
strike-slip and earlier dip-slip motion on the Garlock fault will be examined here on the basis of sedimentary and tectonic evidence from the El Paso basin.

METHODS

During this study, the Miocene strata of the El Paso basin were remapped, and representative lithologies were sampled for petrographic study. Paleocurrent directions were derived from calculated vector means of foreset orientations. Conglomerate compositions were determined by counting approximately 100 clasts in the pebble-to-cobble size range exposed on a single outcrop. Thin-section point counting (Dickinson, 1970) was used to determine sandstone modal compositions, which are presented as Q:F:L ratios. Detailed discussions of these methods are given in Loomis (1984, Appendix III).

A 1,500-m-thick magnetostratigraphic section was sampled through the Dove Spring Formation of the Ricardo Group. Sampling sites were spaced at 10 to 20-m intervals, and at each site, 3–4 oriented specimens were collected. Based on thermal demagnetization studies of pilot specimens (discussed later), all specimens were demagnetized at 450 and 500 °C. The results from the multiple specimens at each site were evaluated using Fisher (1953) statistics and were classified following Johnson and others (1982) as "class I" if Fisher $k > 10$; "class II" if $k < 10$, but two specimens were in close agreement and their polarity was unambiguous; or "class III" if the results were too dispersed for use. The mean site directions were used to calculate the latitude of the virtual geomagnetic pole (VGP) at each sampling level, and α_{95}-error envelopes were calculated for each VGP latitude. The local magnetostratigraphy was defined by magnetic reversals inferred from the changing VGP latitudes.

STRATIGRAPHY OF THE EL PASO BASIN

The fill of the El Paso basin includes clastic sediments of the Paleocene Goler Formation (Dibblee, 1952, 1967; Cox, 1982) and continental
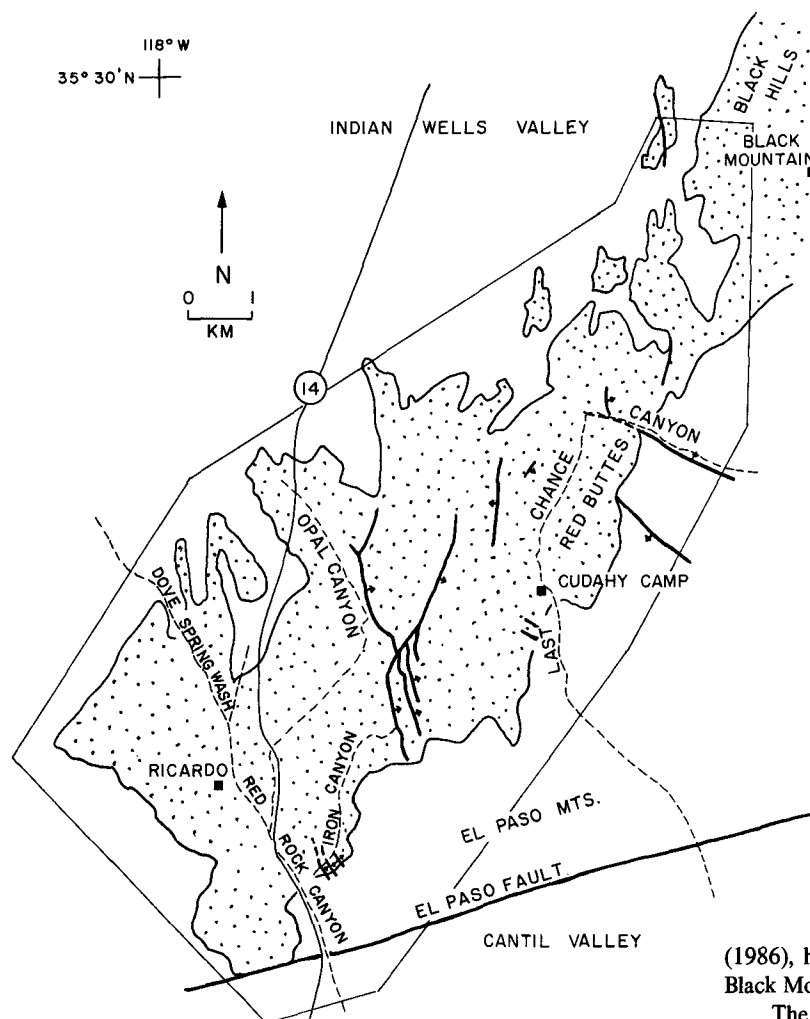
Figure 2. Geographic names and major faults in the El Paso basin area. The stippling denotes the outcrop area of the Ricardo Group. The enclosed box indicates the region encompassed by the geologic map of Figure 3.

sediments and volcanics of the Miocene Ricardo Group (Merriam, 1919; Dibblee, 1952, 1967; Whistler, 1969; Loomis, 1984). Unnamed post-Miocene sediments, at least in part Pleistocene (Dibblee, 1952; Whistler, 1969; Carter, 1980), are also present. Tertiary rocks of the basin onlap southward onto the eroded pre-Tertiary basement complex of the El Paso Mountains (Fig. 1) which includes metasediments, metavolcanics, and Mesozoic granitoid intrusive rocks (Dibblee, 1952; Christiansen, 1961; Cox and Morton, 1980).

The Goler Formation (Figs. 2 and 3) is a 4,300-m-thick assemblage of middle Paleocene conglomerate, sandstone, and mudrock derived primarily from granitic-metasedimentary sources to the east (Cox, 1982). The Goler Formation was tilted to the north and eroded sometime between middle Paleocene and early Micoene time.

The Miocene strata of the El Paso basin were first described by G. K. Gilbert (1875) and subsequently by Baker (1911, 1912), who included them in the Rosamond Series. The names "Ricardo Group" and "Ricardo Formation" were first applied by Merriam (1913, 1919) to the rocks in Red Rock Canyon near the former town of Ricardo (Fig. 2). Dibblee (1952, 1967) mapped the area, divided the Ricardo Formation into eight members, and designated a type area between Red Rock and Last Chance Canyons. A 10.3-m.y. K-Ar age near the base of the Ricardo was determined by Evernden and others (1964) in a study of the isotopic ages of North American land-mammal faunas. Whistler (1969) developed a detailed record of Clarendonian microvertebrates from the Ricardo. The Black Mountain Basalt was named by Baker (1912) and mapped by Dibblee (1952, 1967); both considered it Quaternary. Cox and Diggles
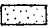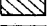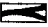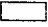
(1986), however, have determined an early Miocene K-Ar age for the Black Mountain Basalt.

The Ricardo Formation of Dibblee (1952, 1967) is divisible into two distinct lithostratigraphic units: a 350-m-thick, lower volcanic unit of andesite, tuff, basalt, and conglomerate which is unconformable on the Paleocene Goler Formation and is equivalent to Dibblee's (1967) members 1 and 2, and a 2,000-m-thick upper unit of conglomerate, sandstone, mudrock, chert, basalt, and tuff, containing Dibblee's (1967) members 3-8 (Fig. 4). K-Ar, fission-track, and magnetostratigraphic dates indicate that these units differ significantly in age and that the disconformity between them represents a hiatus of at least 1.5 m.y. The disconformity or low-angle unconformity separating these units is indicated by the following features: (1) the base of the upper unit contains channels incised into the lower unit, (2) clasts derived from the lower unit are incorporated in conglomerates at the base of the upper one, and (3) the contact between the two units cuts stratigraphically downward to the basement along strike. These two units are sufficiently different lithologically to warrant their definition as separate formations. Consequently, we have elevated Dibblee's (1952, 1967) Ricardo Formation to group status within which two new formations are defined.

The Cudahy Camp Formation (Table 1) supercedes Dibblee's (1967) members 1 and 2. This name is taken from Cudahy Camp in Last Chance Canyon (Fig. 2), where the maximum thickness and type locality (Dibblee, 1952, 1967) of the formation is exposed. This unit contains andesite, tuff, and conglomerate, as well as the Black Mountain Basalt. Cox (1982) sampled the Black Mountain Basalt near the base and top of a sequence of 15 flows exposed on the east slopes of Black Mountain and obtained K-Ar ages of 17.1 ± 0.5 m.y. and 15.1 ± 0.5 m.y., respectively. This isotopic age range places the Black Mountain Basalt in the early middle to early Miocene. K-Ar ages have also been obtained on two andesite flows in the Cudahy Camp Formation (Cox and Diggles, 1986). The upper andesite,

LEGEND

QUATERNARY { ALLUVIUM, TERRACES, LANDSLIDES

MIOCENE {
RICARDO GROUP : UNDIVIDED

DOVE SPRING FM. {
MEMBER 5
MEMBERS 2-4
MEMBER 1

CUDAHY CAMP FM. {
BLACK MTN. BASALT
BASALT DIKES
MEMBERS 2-4
MEMBER 1

PALEOCENE { GOLER FM. : UNDIVIDED

MESOZOIC { GRANITOID COMPLEX

PALEOZOIC { METASEDIMENTARY AND METAVOLCANIC ROCKS

0.5   0   1 KM

N

Figure 3. Geologic map of the El Paso basin and the El Paso Mountains. The geographic location of the map is shown in Figure 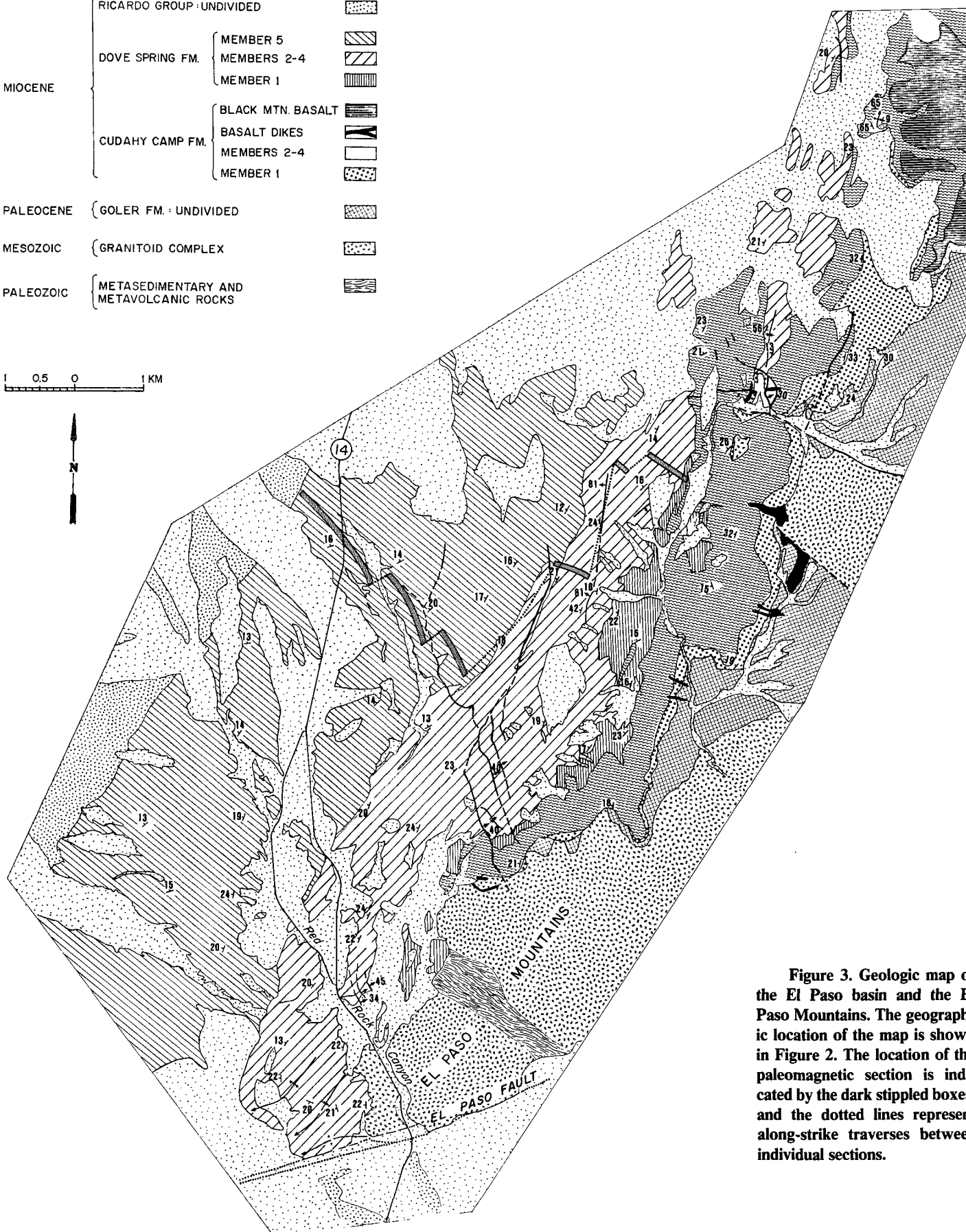2. The location of the paleomagnetic section is indicated by the dark stippled boxes, and the dotted lines represent along-strike traverses between individual sections.
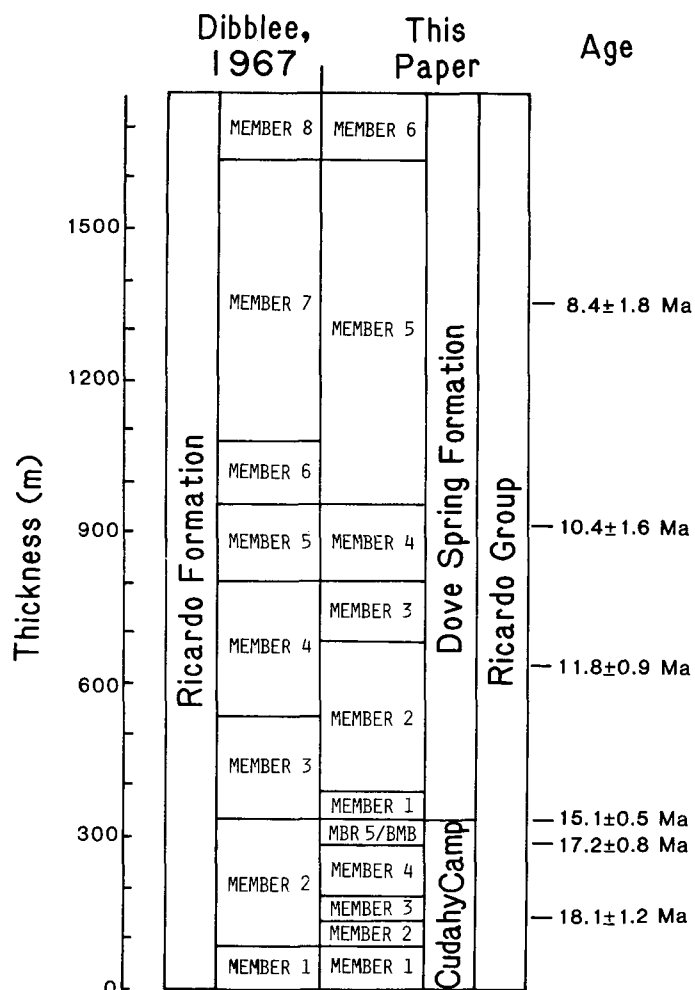
Figure 4. Correlations between Dibblee's (1952, 1967) lithostratigraphic terminology and the new definitions used in this paper. Radiometric dates are shown at their appropriate stratigraphic position. See text for description of each member.

member 5, has been dated at 17.2 ± 0.5 m.y., and the age of the lower andesite has been determined to be 18.1 ± 0.6 m.y. Both ages are early Miocene (Palmer, 1983; Berggren and others, 1985). The age of the basal conglomerate (member 1; see Table 1) is unknown, but it is probably also early Miocene.

The newly named Dove Spring Formation (Table 1) encompasses Dibblee's members 3–8 and is unconformable on the Cudahy Camp Formation. The name is taken from Dove Spring Wash (Fig. 2) where the upper 800 m of the Ricardo Group is well exposed. The Dove Spring Formation is middle to late Miocene in age, and it consists of conglomerate, sandstone, mudrock, chert, basalt, and tuff. Member 6 of the Dove Spring Formation is composed of poorly exposed, weakly consolidated, and gently dipping to flat-lying sedimentary rocks. A disconformity may be present between member 6 and the underlying 1,500 m of Ricardo strata. The presence of well-developed caliches and silcretes near the top of member 5 suggests that increasingly sporadic sedimentation preceded the initial deposition of member 6. Due to its poor exposure, member 6 was not included in our analysis. The type section for the Dove Spring Formation is located between Red Rock and Last Chance Canyons (Fig. 2) and

is the same as that designated by Dibblee (1952, 1967) for his Ricardo members 3–8. The Dove Spring strata are exposed in a northeast-striking homocline dipping 15°–20° northwest. They are overlain by fossiliferous lacustrine silt and clay of unknown Pleistocene age (Whistler, 1969), by alluvial fanglomerates, and by elevated, dissected post-Miocene terrace gravels also assumed to be Pleistocene (Dibblee, 1952).

MAGNETOSTRATIGRAPHIC AGE OF THE DOVE SPRING FORMATION

Due to the abundance of volcanic breccias, conglomerates, and thick ash-flow tuffs, extensive magnetic sampling was not undertaken in the Cudahy Camp Formation. More than 100 magnetic sampling sites (Fig. 3), however, were placed in the Dove Spring Formation in an attempt to develop a magnetostratigraphy for these strata. Stepwise thermal demagnetization of numerous pilot specimens revealed similar magnetic behavior for most specimens. Typical results (Fig. 5) show the following characteristics: (1) large changes in intensity below ~250 °C and, for specimens with a reversed depositional remanence (DRM), an increase in intensity; (2) between 250 and 500 °C, a slow decrease in the remanent intensity, and in some cases (for example, specimen R103A, Fig. 5), no significant change in intensity within this temperature range; and (3) between 550 and 600 °C, a very rapid decrease in intensity. For all specimens, the characteristics remanence directions are displayed between 250 and 500 °C.

We interpret these data as indicating the presence of a low-temperature normal overprint that is removed below ~200 °C and is responsible for the increase in intensity observed in the reversed specimens. The rapid decrease in intensity above 550 °C suggests that the primary magnetic carrier is magnetite. Furthermore, the slow to negligible decrease in intensity between 250 and 500 °C suggests that this magnetite is primarily fine grained. Because this uncomplicated demagnetization behavior typifies most Dove Spring samples, all other specimens were demagnetized at 450 and 500 °C in order to reveal their characteristic remanence and to minimize the effects of secondary overprinting. Following this treatment, the grouped magnetic data passed the reversal test and displayed a mean of 15° of counterclockwise rotation (Fig. 6).

The magnetic polarity stratigraphy (MPS) based on the demagnetized and statistically evaluated data from each site is shown in Figure 7. The error envelope on the VGP latitude emphasizes the generally unambiguous polarity data throughout the section. The most striking feature of the Dove Spring MPS is the long interval of normal polarity between 600 and 1,200 m (N8 and N9, Fig. 7). Because of the Clarendonian fossils present in the Dove Spring strata, this long normal interval should correlate with the normal segment of magnetic chron C5N (Berggren and others, 1985) spanning 8.92 to 10.42 Ma (Fig. 7) in the magnetic polarity time scale (MPTS). Fission-track dates of 8.4 ± 1.8 Ma and 10.4 ± 1.6 Ma (Cox and Diggles, 1986) also support this correlation. Given this correlation, magnetozones R1 to R8 can be correlated with chrons C5AB to C5R (13.46–10.42 Ma). The presence in the local Dove Spring MPS of all but one of the well-documented magnetozones in this time span lends support to the interpretation proposed here. Statistical evaluation based on the formulations of Johnson and McGee (1983) indicates that the portion of the magnetostratigraphy below the long normal magnetozone (Chron C5N) should encompass at least 2.5 m.y. In addition, a fission-track date of 11.8 ± 0.9 (2σ) Ma on a volcanic ash at 370 m (Fig. 7) is in basic agreement with this correlation.

The interpretation of magnetozones R10 to N13 is less straightforward than in the underlying strata. The most reasonable interpretation of the MPS, however, correlates magnetozones R10–N11 with chrons 9 and

TABLE 1. STRATIGRAPHY OF THE DOVE SPRING AND CUDAHY CAMP FORMATIONS

| Formation	Member	Thickness (m)	Description	Age m.y.	Basal contact	Location
Dove Spring	6	500	Weakly consolidated, unstratified clay; arkosic sand; coarse gravel; and boulders.	<7	Disconformable	Opal Canyon, Dove Spring Wash
Dove Spring	5	700	Yellowish gray to pale orange plutonic-volcanic pebble conglomerate; coarse to fine lithic arkose and arkose; gray, light brown, and green mudrock; pinkish gray limestone; light gray to green, bedded and nodular chert; and volcanic ash and tuff. Numerous, well-developed caliches near top.	10.5–7	Conformable	Opal Canyon, Red Rock Canyon
Dove Spring	4	60–150	Basalt and massive, planar-bedded, and cross-bedded medium-to coarse-grained lithic sandstone; gray to green mudrock, limestone, and chert; base and top marked by pairs of basalt flows.	11.5–10.5	Conformable	Last Chance Canyon, Red Rock Canyon
Dove Spring	3	100–125	Massive to planar-bedded medium-grained sandstone, siltstone, gray and green mudrock, and chert; poorly sorted volcanic and plutonic conglomerate and cross-bedded coarse lithic sandstone.	12.5–11.5	Conformable	Last Chance Canyon, Red Rock Canyon
Dove Spring	2	200–245	Pale red to light yellowish gray, poorly sorted, volcanic-plutonic pebble conglomerate; massive to cross-bedded, coarse, poorly sorted lithic sandstone, and tuff-breccia in southwest; planar-bedded to massive lithic sandstone, green mudrock and chert, with limestone, tuff, and volcanic ash in the northeast.	13.3–12.5	Conformable	Last Chance Canyon
Dove Spring	1	0–280	Yellowish gray to reddish purple, poorly sorted, massive to crudely stratified volcanic-cobble roundstone conglomerate, and massive and cross-bedded lithic sandstone.	~13.5–13.3	Angular unconformity	Last Chance Canyon; pinches out to northeast and southwest.
Cudahy Camp	Black Mountain Basalt		Olivine basalt, as many as 15 separate flows.	15.1 ± 0.5– 17.1 ± 0.5 (Cox, 1982)	Possible unconformity	Black Hills and Black Mountain
Cudahy Camp	5		Blackish to grayish red, massive and flaggy andesite flows.	17.2 ±0.5 (Cox and Diggles, 1986)	Conformable	Last Chance Canyon to the Black Hills
Cudahy Camp	4	0–150	Grayish yellow to pinkish gray, massive tuff breccia.		Conformable	Black Mountain to Cudahy Camp in Last Chance Canyon; pinches out west of Last Chance Canyon
Cudahy Camp	3	0–50	Red-purple to dark reddish brown andesite in brecciated and massive flows.	18.1 ± 0.6 (Cox and Diggles, 1986)	Conformable	Last Chance Canyon; pinches out southwest and northeast along strike.
Cudahy Camp	2	0–80	White to light yellowish gray–bedded, waterlain sandy tuff and pink or grayish yellow tuff-breccia. Base defined by light colored, bedded tuff up to 2 m thick with occasional ripple marks and shrinkage crack casts; contains pink, massive tuff-breccia containing primarily 1- to 5-mm clasts of pumice and banded felsite.		Conformable	Last Chance Canyon
Cudahy Camp	1	0–180	Red or gray diamictic conglomerate of rounded polylithologic boulders and cobbles in coarse arkosic sand; prominent channels at base. Weakly cemented and poorly exposed.	>18.1	Angular unconformity	Maximum thickness at Black Mountain and in Last Chance Canyon; thins eastward (Dibblee, 1967; Cox and Diggles, 1986) and to the southwest.
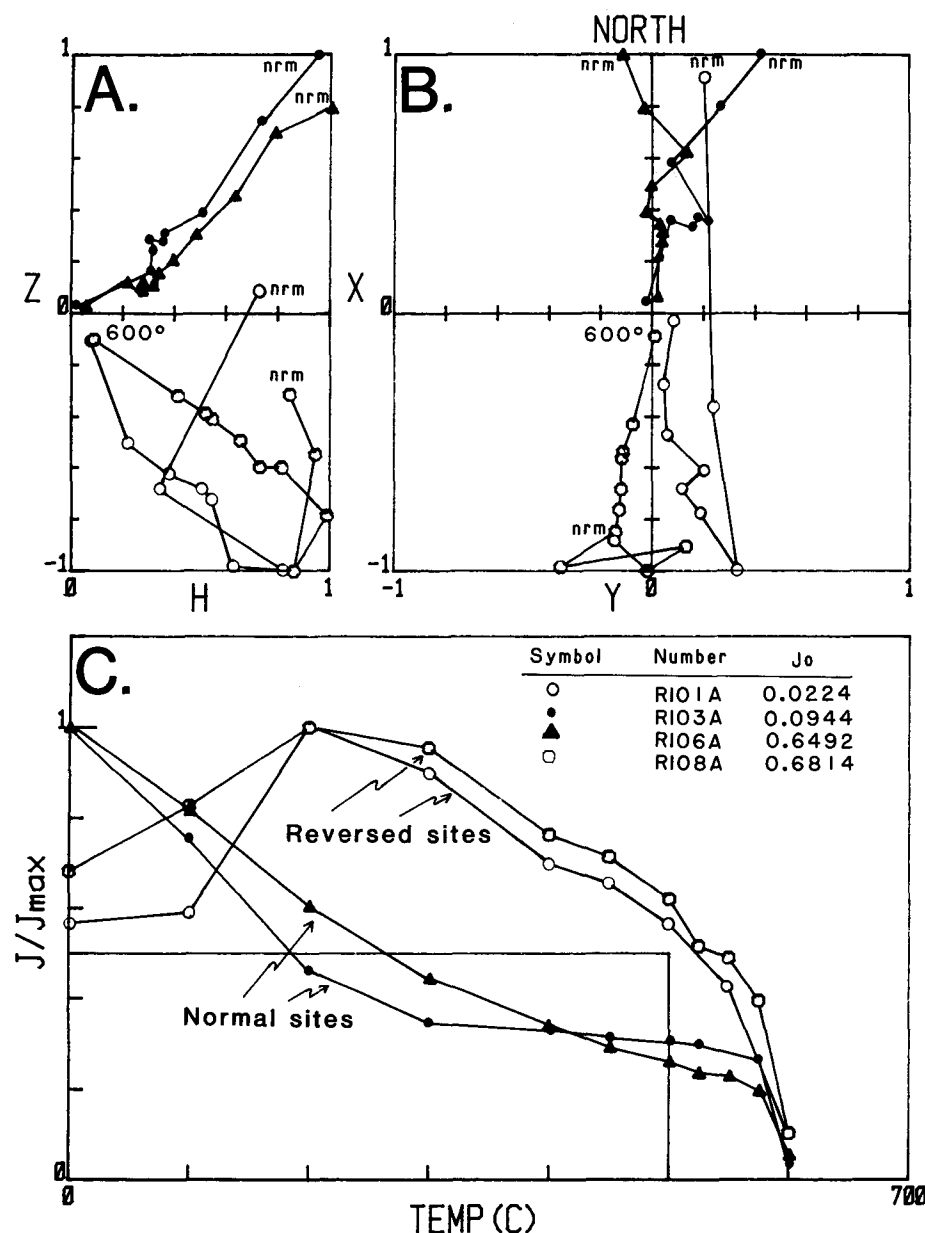
Figure 5. Typical thermal demagnetization behavior for siltstones in the Dove Spring Formation. Solid symbols, normal polarity specimens; open symbols, reversed polarity specimens. A. Magnetic inclination. Univectorial decay toward the origin is shown by all specimens at temperatures above 200 °C. B. Magnetic declinations. Declination plots show antipodal orientations for normal and reversed specimens, following removal of a normal overprint. C. Magnetic intensity (J) during thermal demagnetization. The intensity increase in reversed specimens is due to removal of a normal overprint below ~200 °C. The major drop in intensity between 550 and 600 °C indicates that the primary magnetic carrier is magnetite. Characteristic remanence is displayed between 200 and 550 °C.

10 (8.92–7.90 Ma, Berggren and others, 1985) and magnetozones R12–N13 with chrons 7 and 8 (7.90–6.85 Ma, Fig. 7). An imperfect match between the local MPS and the MPTS, such as displayed here, is not unexpected in a continental environment (Johnson and McGee, 1983) due to both the sporadic nature of deposition and the relatively large spacing (10–20 m) between sampling sites. Despite these caveats, the local MPS, the corroborative radiometric dates, and statistical analysis of the data indicate that the Dove Spring Formation (members 1–5) spans an interval from ~13.5 Ma to ~7.0 Ma. This places the initiation of Dove Spring sedimentation ~3 m.y. earlier than previously believed (Evernden and others, 1964) and extends it 1–2 m.y. later into the late Miocene. The hiatus between eruption of the upper flows of the Black Mountain Basalt and the inception of Dove Spring deposition is ~1.5 m.y., whereas the span between member 5 of the Cudahy Camp Formation and the Dove Spring is ~3.5 m.y. Member 6 of the Dove Spring Formation is constrained to be younger than 7 m.y., but at present, no reliable estimates of the time encompassed by these largely unexposed strata can be made.

SEDIMENT-ACCUMULATION RATES

Sedimentation-accumulation and subsidence histories for the Dove Spring Formation are shown in Figure 8. Packets of sediments defined by magnetozone boundaries have been decompacted using the methods of Sclater and Christie (1980). During these calculations, it was assumed that an additional 500 m of strata were deposited prior to uplift of the section. Decompacted, "instantaneous" sediment-accumulation rates averaged over 1- to 2-m.y.-long intervals for deeply buried strata are up to twice as large as the rates calculated from presently preserved thicknesses. By decompacting the sedimentary column after incremental removal of successive layers, it is possible to develop a subsidence history for the basin during Dove Spring deposition (Fig. 8). Each of these depictions (subsidence and compacted or decompacted accumulation) show four discrete intervals of sedimentation. Accumulation was rapid from about 13.5 to 12.0 Ma, corresponding approximately to deposition of the conglomerates and sandstones of members 1 and 2. These rates slowed somewhat during
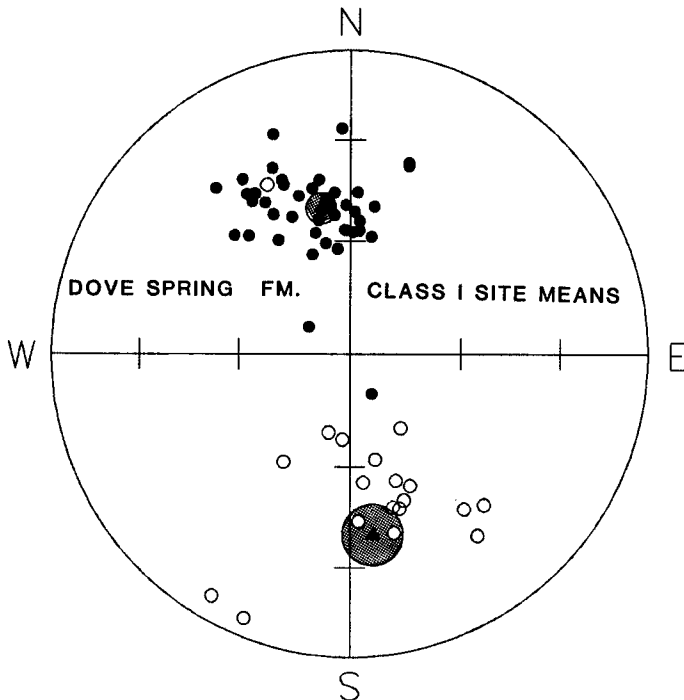
Figure 6. Stereonet plot of demagnetized class I normal and reversed sites. The data are nearly antipodal and indicate that a mean of 15° of counterclockwise rotation has occurred. The stippled areas indicate the α_{95}-error envelope on the mean directions.

the succeeding 2 m.y. (members 3 and 4) but increased sharply between 10.4 and 9 Ma, corresponding to about the lower 600 m of member 5. The predominantly fine-grained upper 300 m accumulated at a slower rate from 9 Ma on.

DETRITAL COMPOSITION

The sandstones and conglomerates of the Ricardo Group were subdivided into four major compositional petrofacies, using petrographic and field techniques for determining detrital composition (Loomis, 1984). All of the sandstones are texturally and compositionally immature. The distribution of compositional petrofacies is in large part stratigraphically controlled (Fig. 9). In stratigraphic order, these petrofacies are (1) plutonic-sedimentary-metamorphic conglomerate and lithic sandstone, (2) volcanic conglomerate and lithic sandstone, (3) mixed volcanic-plutonic conglomerate and lithic arkose, and (4) granitoid plutonic conglomerate and alkali feldspar arkose (Table 2). The compositions of these four facies are shown graphically in Figure 10.

PALEOCURRENTS

Paleocurrent directions in the Dove Spring Formation were determined by statistical analysis of field measurements of the azimuths of 222 cross-beds. Measurements were taken at 44 locations throughout the study area, and data from individual stations were grouped by detrital petrofacies and by age (stratigraphic member) to test for systematic changes in current direction with time and source area. No other current indicators were sufficiently abundant to provide reliable data. Similarly, paleocurrent directions were not quantitatively determined for the Cudahy Camp Formation, because current indicators are too rare for statistical analysis.

Paleocurrent directions show a strong preferred orientation toward the northwest to north-northwest throughout the Dove Spring Formation, except in the uppermost strata of member 5 (Figs. 11a and 12), and there is essentially no systematic variation in paleocurrent direction with time (Figs. 11b–11d). Similarly, the described petrofacies, which might be expected to reflect geographically distinct source areas, show no significant paleocurrent differences between them (Figs. 11e, 11f). The relatively small, postdepositional, counterclockwise rotation of the Dove Spring strata shown by the magnetic data (Fig. 6) indicates that only a minor clockwise correction (~15°) needs to be added to the presently observable vectors in order to reconstruct former current directions.

DETRITAL PROVENANCE

Plutonic-Sedimentary-Metamorphic Clasts

The basal unit of the Cudahy Camp Formation which contains polylithologic conglomerate and lithic sandstone has few paleocurrent indicators. An estimate of approximately northward paleoflow can be made on the basis of qualitative observations: (1) maximum clast size in the basal conglomerate decreases northward, and (2) measurements from pebble imbrications in Cudahy Camp member 1 on the east slopes of Black Mountain (Cox and Diggles, 1986) indicate northward paleocurrents in that area.

Possible sources for all the distinctive detrital lithologies in this petrofacies can be found within the El Paso basin and El Paso Mountains to the south. Many quartzite, black chert, metavolcanic, and metasedimentary clasts common in the Cudahy Camp Formation appear to be recycled from the underlying Goler Formation. Clasts derived from the Garlock Formation, the Mesquite Schist, and granophyre exposed in the western El Paso Mountains are also common in the Cudahy Camp basal conglomerate. In sum, rapid fining to the north, the presence of clasts up to 1 m in diameter in the more southerly outcrops, and the nearby availability of appropriate clast lithologies suggest that the basal Cudahy Camp Formation was locally derived from the pre-Miocene rocks exposed along the present-day El Paso Mountains.

Volcanic Clasts

Paleocurrent indicators in the volcanic petrofacies clearly show derivation from the south-southeast (Figs. 11f and 12). Volcanic-clast conglomerates in the Dove Spring Formation are characterized by subrounded to rounded clasts of porphyritic andesite, banded felsite, vesicular basalt, and pumiceous tuff. Although the Cudahy Camp Formation is now exposed to the southeast, volcanic detritus in the Dove Spring (with the exception of the basal 0.5 m) is unlike the andesites and tuffs of the Cudahy Camp. Consequently, it is necessary to look farther south for the source of volcanic clasts in the Dove Spring Formation. The Tertiary rocks of the Mojave block, south of the Garlock fault, contain large volumes of volcanic rocks, including all of the major clast lithologies in Dove Spring conglomerates. The occurrence of similar Tertiary volcanics over large areas of the western Mojave Desert makes it difficult to locate the specific source area of clasts in the Dove Spring, and the task is further complicated by uncertainty about the Miocene position of the El Paso basin along the Garlock fault. Nevertheless, the volcanic detrital source was clearly in the northern Mojave block south of the Garlock fault, on a line between the present longitude of the El Paso basin and its longitude in the late Miocene, which may have been as much as 64 km farther east along the Garlock fault.

LITHOLOGIC CHARACTER

VIRTUAL GEOMAGNETIC POLE LATITUDE

MAGNETIC POLARITY STRATIGRAPHY

MAGNETIC POLARITY TIME SCALE

THICKNESS (meters)

MILLION YEARS

CLASS I DATA •
CLASS II DATA o

• NORMAL POLARITY
o REVERSED POLARITY

ALPHA-95 LIMITS

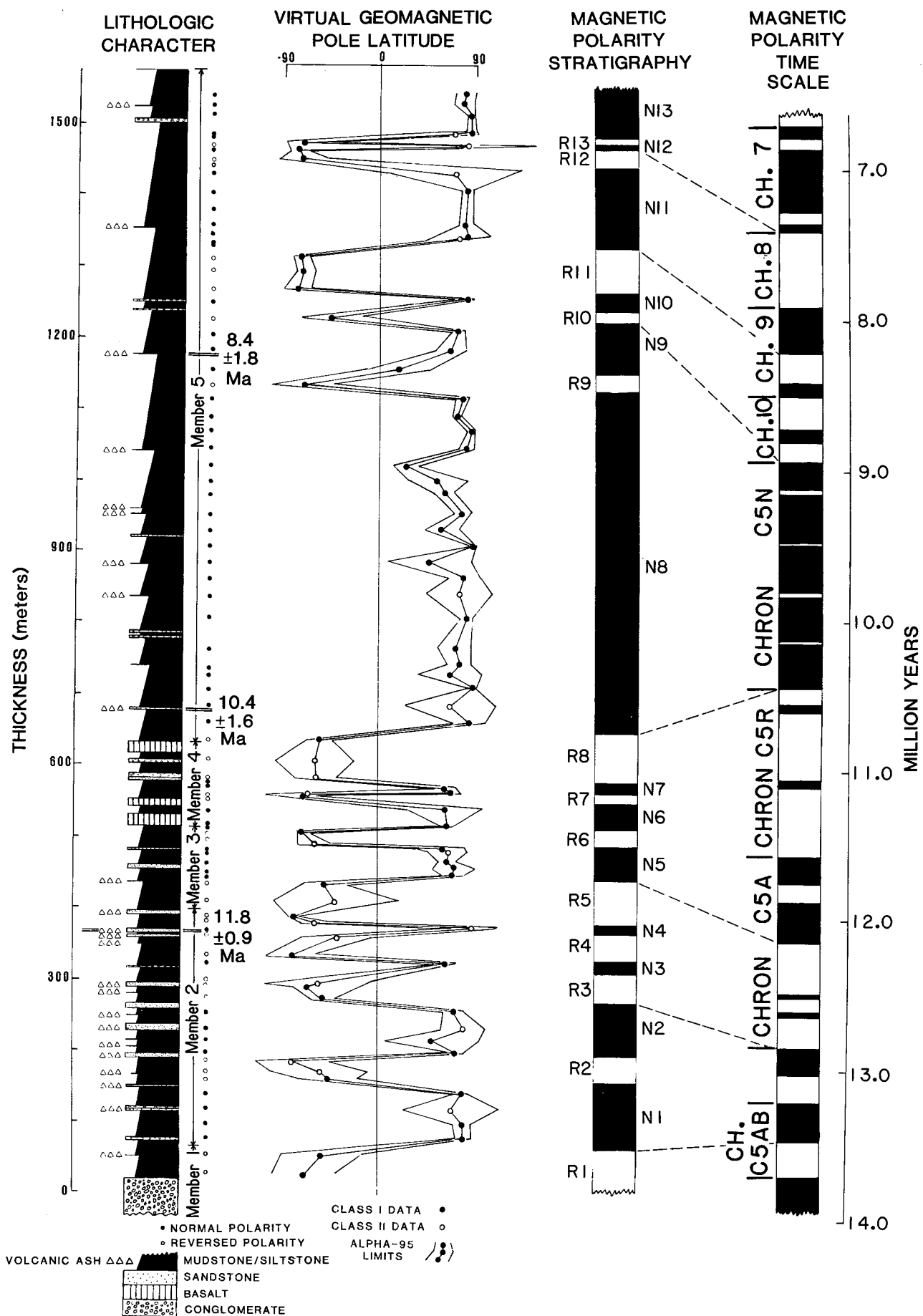VOLCANIC ASH △△△

MUDSTONE/SILTSTONE
SANDSTONE
BASALT
CONGLOMERATE

Figure 7. The lithostratigraphy, VGP latitudes, fission-track dates, and magnetic polarity stratigraphy (MPS) of the Dove Spring Formation, members 1–5, and their correlation with the magnetic-polarity time scale (Berggren and others, 1985). Only sandstone and conglomerate units thicker than ~5 m are depicted in the lithostratigraphy. Generally unambiguous polarities are indicated by the α_{95}-error envelope on the individual VGP latitudes. The local MPS is based on the VGP latitudes. The numbered magnetozones (R1, N1, etc.) are referred to in the text. Numerous volcanic ashes (triangles) occur in the section, and fission-track dates of 11.8 ± 0.9 (2σ) Ma at 370 m (this study), of 10.4 ± 1.6 Ma at 680 m (Cox and Diggles, 1986), and of 8.4 ± 1.8 Ma at 1,180 m (Cox and Diggles, 1986) aid in the correlation. The long normal magnetozone from 650–1,200 m (N8, FN9 of Fig. 7) is correlated with marine anomaly 5 or magnetic chron C5N. A reliable match of the MPS with the MPTS appears possible for magnetozones R1 to R8 (~13.5 to 10.4 Ma). The fission-track dates at 370 and 680 m support this correlation. Correlation of magnetozones R10 to N13 is more ambiguous, but the most reasonable match places the top of Dove Spring member 5 at ~7 Ma.

RICARDO GROUP PETROFACIES

4 GRANITOID PLUTONIC CONGLOMERATE AND ALKALAI FELDSPAR ARKOSE

3 VOLCANIC-PLUTONIC CONGLOMERATE AND HIGH-QUARTZ LITHIC ARKOSE

2 VOLCANIC-CLAST CONGLOMERATE AND LOW-QUARTZ LITHIC SANDSTONE

1 PLUTONIC-SEDIMENTARY CONGLOMERATE AND LITHIC SANDSTONE

VOLCANIC ROCKS

TIME-MARKER

TABLE 2. PETROFACIES DATA FROM THE RICARDO GROUP

Petrofacies		Composition	
Name	No.	Q:F:L* (sandstones)	P:V:S:M† (conglomerates)
Plutonic-sedimentary-metamorphic conglomerate and lithic sandstone	1	46:32:22	39:4:9:48
Volcanic conglomerate and lithic sandstone	2	11:25:64	2:95:2:1
Mixed plutonic-volcanic conglomerate and lithic arkose	3	35:44:21	22:63:2:13
Alkali feldspar arkose	4	40:59:1	n.a.

*Percentages of quartz (Q), feldspar (F), and lithic (L) grains.
†Percentage of plutonic (P), volcanic (V), sedimentary (S), and metamorphic (M) clasts.
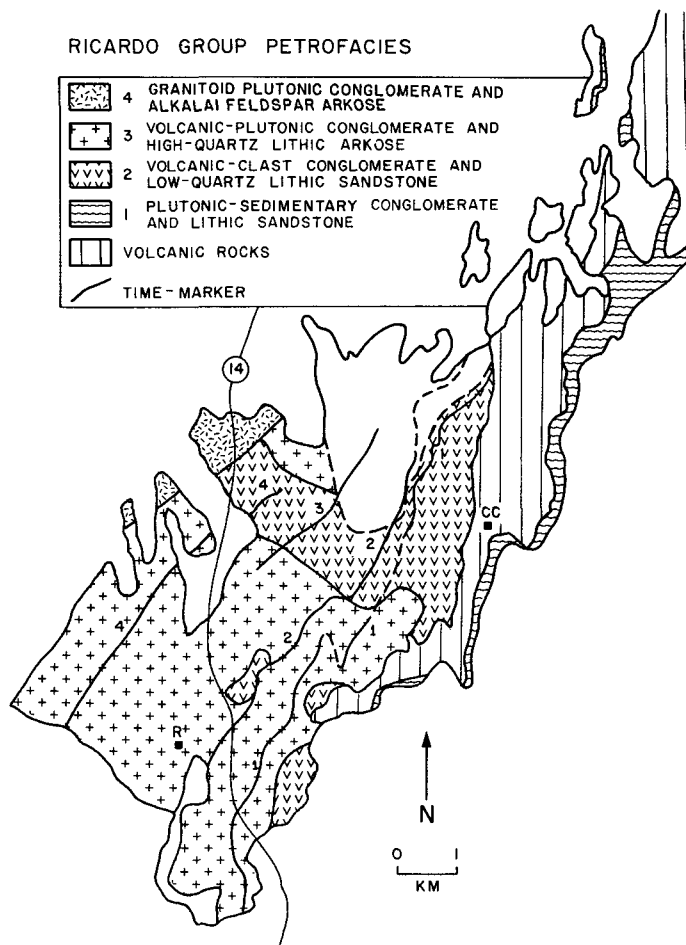
Figure 9. Sandstone and conglomerate petrofacies in the Ricardo Group. Time markers shown are 1, tuff-breccia in Dove Spring Formation member 2; 2, base of lower basalt in member 4; 3 and 4, ash beds in member 5. CC, Cudahy Camp; R, Ricardo.

OBSERVED THICKNESS
DECOMPACTED, NORMALIZED THICKNESS
BASE OF THE DOVE SPRING FM.
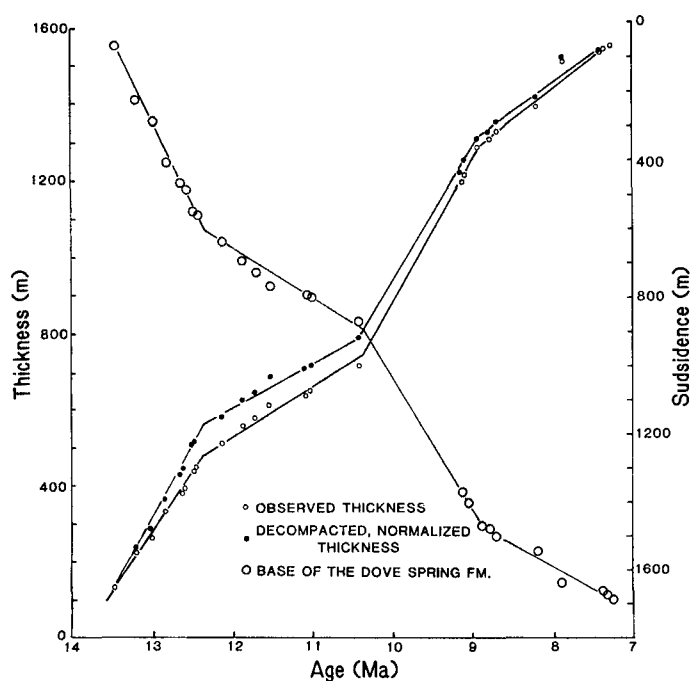
Figure 8. Sediment-accumulation and subsidence curves for the Dove Spring Formation based on the correlation of the local MPS with the MPTS. Open, small circles show presently observed thickness versus time relationships. The solid circles represent decompacted thicknesses based on the formulations of Sclater and Christie (1980) and assuming an additional 500 m of post–7 Ma sediments have been eroded. After the total decompacted thickness is normalized to the presently observed thickness, the slope is proportional to the long-term "instantaneous" sediment-accumulation rate, that is, the rate that prevailed at the time of deposition. Decompaction enhances the "instantaneous" rates in the more deeply buried, more compacted sediments. The large open circles delineate the subsidence history of the base of the Dove Spring Formation. By 7.2 Ma, more than 1,600 m of sediments had accumulated since 13.5 Ma. Subsequent addition of 500 m of strata compacted these underlying strata to their present thickness. The inflection points on all curves at ~10.5 and ~9 Ma can be interpreted as responses to nearby tectonic events.
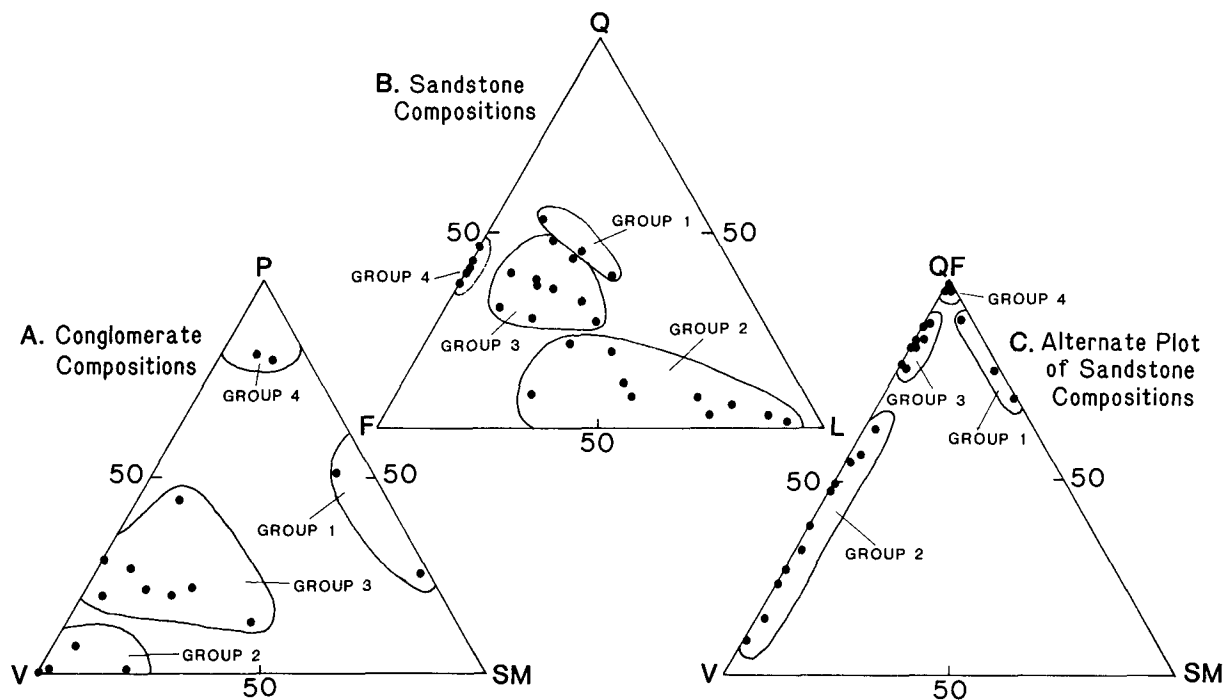
Figure 10. Sandstone and conglomerate modal compositions, Ricardo Group; see text for discussion. Group 1, plutonic-sedimentary-metamorphic petrofacies; group 2, volcanic petrofacies; group 3, volcanic-plutonic petrofacies; group 4, granitoid-plutonic petrofacies.

Volcanic-Plutonic Clasts

Streams which deposited clastic rocks of the volcanic-plutonic petrofacies flowed from the south-southeast as in the volcanic-clast petrofacies (Figs. 11e and 12), and volcanic detritus in this petrofacies is identical to that observed in the more volcanic-rich facies. This facies, however, contains a higher proportion of plutonic, metamorphic, and sedimentary cobbles and of quartz and feldspar grains, which predominate over volcanic-rock fragments. The appearance of plutonic clasts and the greater abundance of quartz in this facies suggest a change to a more plutonic-rich source area, but it is not accompanied by a change in paleocurrent direction or in the lithology of the volcanic fraction of the sediment. Because this petrofacies is in general younger than the volcanic-rich facies described above, this change in sediment composition may be due to eventual exposure of basement rocks in the source area by deep erosion, while the volcanic cover also continued to erode. Granitoid plutonic rocks that could constitute a possible sediment source are exposed beneath eroded Tertiary cover over wide areas of the Mojave Desert, but clasts from the Dove Spring Formation are not sufficiently distinctive to match to a unique source.
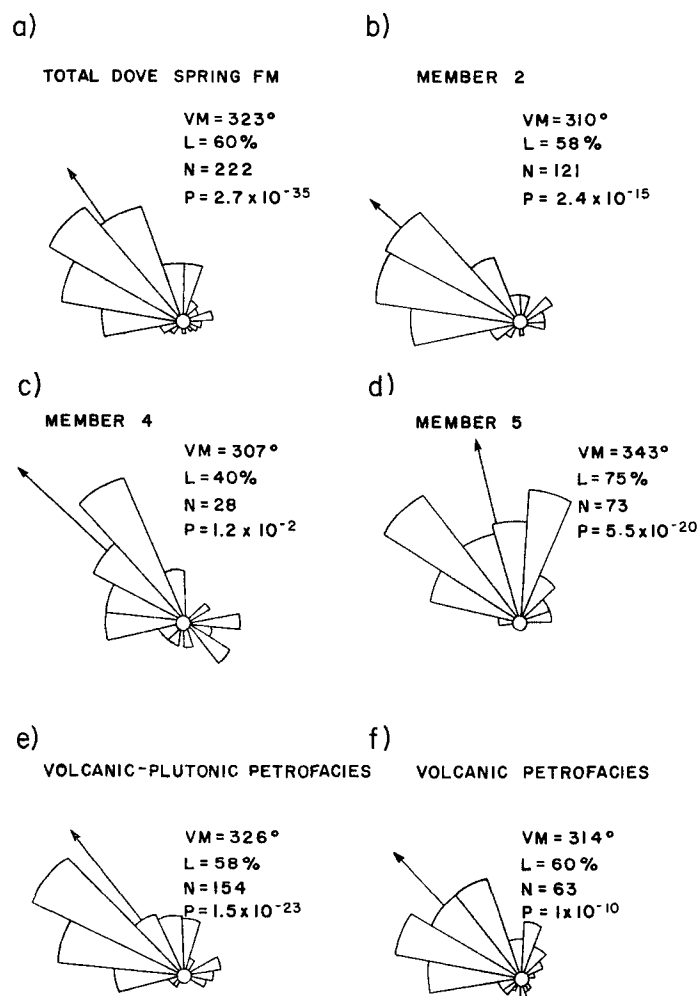
Granitoid Plutonic Clasts

Although the granitoid plutonic petrofacies is exposed only at the top of the Dove Spring Formation in members 5 and 6, it is tectonically significant, because it is compositionally unrelated to the rest of the Dove Spring strata. Few paleocurrent data are available from sandstones in this petrofacies, but lithologic and stratigraphic criteria suggest that the source of sediment in this petrofacies was entirely different from sources for other

Dove Spring clastics. The absence of unstable lithic grains in this facies and the high proportion of alkali feldspar and quartz indicate a probable granitic source for this sediment. The interbedded conglomerates are dominated by clasts of microcline-biotite granite and granodiorite containing dark, schistose xenoliths. The boulders increase to more than 1 m diameter in member 6 updip and west of the member 5 arkoses. The westward coarsening, large clast sizes, and available paleocurrent data suggest that the arkoses and associated boulders were derived from the west. Granites and xenolith-bearing granodiorites of the Sierra Nevada (Samsel, 1962), exposed as close as 4 km west of outcrops of the Dove Spring Formation, are the most likely source for this petrofacies.

STRUCTURAL GEOLOGY

The structural geology of the El Paso basin is typical of the Basin and Range region north of the Garlock fault. The western boundary of the basin, formed by the Sierra Nevada fault, coincides with the western limit of basin-and-range structures. The spatial and temporal pattern of folding, dike injection, and faulting in the study area (Fig. 3) provide important controls on the Miocene history of the El Paso basin.

The Goler Formation was tilted homoclinally to the north and eroded prior to the inception of Miocene sedimentation. More precise time constraints for this deformation are not presently available. Two east-west–trending faults east of Red Buttes (Fig. 2) are the only faults of this orientation in the mapped area (Fig. 3). These steeply dipping faults, which juxtapose a large block of pre-Tertiary basement against the Goler Formation, were active in the middle Paleocene during deposition of the Goler Formation (Cox, 1982). The western edge of the upfaulted basement block is buried by the Cudahy Camp Formation, and so major fault

a)

TOTAL DOVE SPRING FM

VM = 323°
L = 60%
N = 222
P = 2.7 x 10⁻³⁵

b)

MEMBER 2

VM = 310°
L = 58%
N = 121
P = 2.4 x 10⁻¹⁵

c)

MEMBER 4

VM = 307°
L = 40%
N = 28
P = 1.2 x 10⁻²

d)

MEMBER 5

VM = 343°
L = 75%
N = 73
P = 5.5 x 10⁻²⁰

e)

VOLCANIC-PLUTONIC PETROFACIES

VM = 326°
L = 58%
N = 154
P = 1.5 x 10⁻²³

f)

VOLCANIC PETROFACIES

VM = 314°
L = 60%
N = 63
P = 1 x 10⁻¹⁰

Figure 11. Paleocurrent rose diagrams for entire Dove Spring Formation (a), and separately for members 2, 4, and 5 (b–d) and by petrofacies (e–f): see text for discussion. VM, vector mean azimuth; L, vector length (percent); N, population size; p, Rayleigh test value.

be constrained to a precise time interval, and, therefore, they do not offer an independent check on the inferred stress regime.

Within the study area, the Dove Spring Formation and older strata are cut by several significant north-south–striking, low-angle, normal faults (Figs. 2 and 3). The slip surfaces of these faults generally dip at 30°–40° to the east, and ~200–400 m of demonstrable stratigraphic separation is displayed by each fault. Dove Spring members 1–4 and the basal half of member 5 are cut by one or more of these faults. Strata as young as 9–8 m.y. old have therefore been extended in an east-west direction. We attribute the apparent lack of faults within the upper strata of member 5 to the limited exposures of these strata in the northwestern part of the study area rather than to an absence of faulting; therefore, the timing of movement along the north-south normal faults can only be constrained to include strata at least as young as 9 m.y. This east-west extension may have been coeval with activity on the northeast-trending faults. The largest such fault shows down-to-the-southeast displacement and may also have ac-
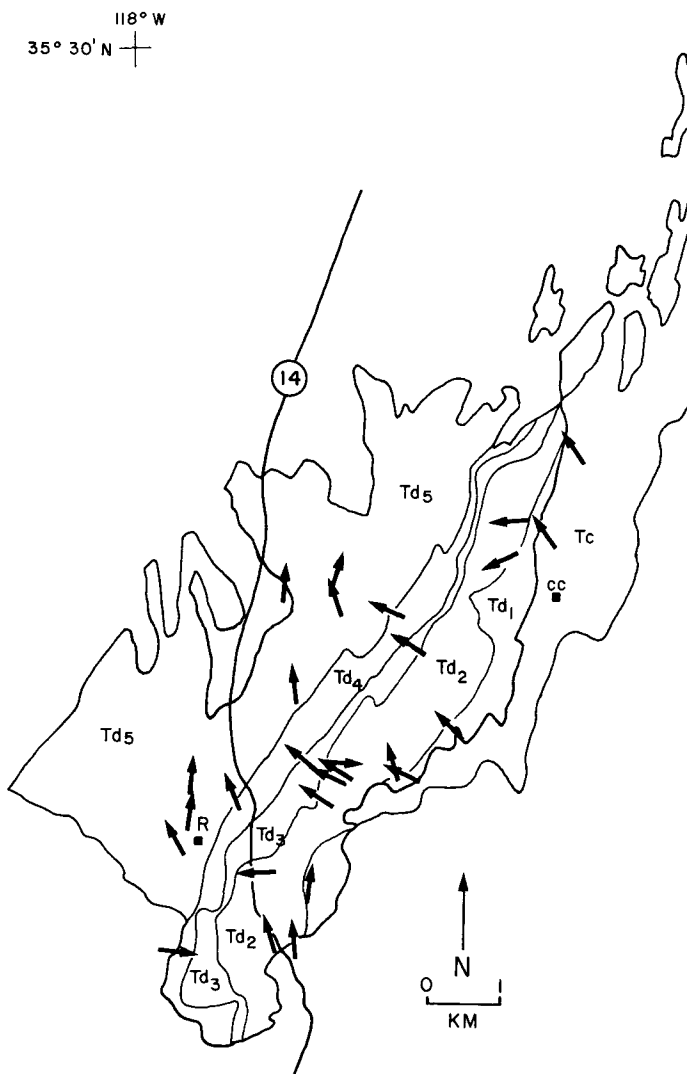
displacement was pre-Miocene. Cox (1982), however, reported that a large basalt dike of presumed early Miocene age that is intruded along the trace of the southern fault is also sheared along the fault, indicating some reactivation following emplacement of the dike.

Both the Goler Formation and the early Miocene Cudahy Camp Formation are cut by a series of vertical east-west–trending dikes (Fig. 3). These dikes cut units as high stratigraphically as member 4 of the Cudahy Camp Formation but do not disrupt the Dove Spring Formation. Intrusion of the dikes apparently followed eruption of member 4 and was approximately contemporaneous with eruption of the Black Mountain Basalt, which is itself underlain by similar dikes (Cox, 1984). The proximity and petrographic similarity of these dikes to the Black Mountain Basalt make them likely sources for the extrusive basalt.

Because dikes and fractures are most likely to form normal to σ_3 (Nakamura and others, 1977), the dikes in the Cudahy Camp Formation probably formed in a north-south tensional regime. Although numerous other local faults cut strata older than the Black Mountain Basalt, none can
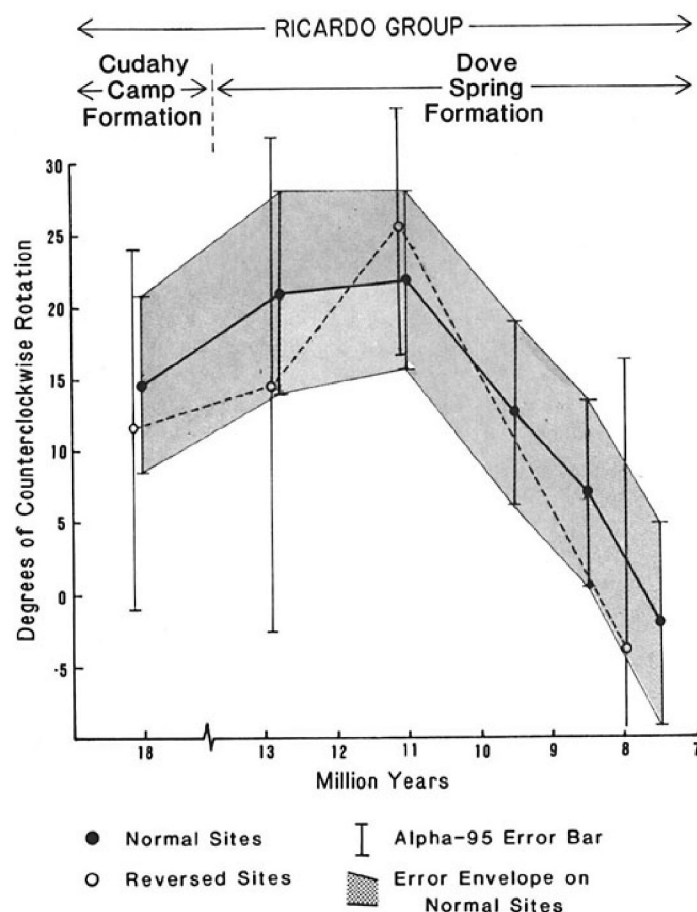
Figure 12. Vector mean paleocurrent orientation at 44 sample sites, Dove Spring Formation.

Figure 13. Counterclockwise rotation of the Dove Spring Formation between 13.5 and 7 Ma. Normally and reversely polarized data are grouped separately for successive age brackets. The error envelope represents a 2 σ confidence interval on the normally polarized data. Strata older than ~10 m.y., including those of the underlying Cudahy Camp Formation, are rotated 15°–20°. Younger strata show progressively lesser amounts of rotation, such that the 7- to 8-m.y.-old beds appear unrotated.

commodated left-slip offset, both of which are consistent with the geometrical constraints imposed by nearby north-south normal faults.

The El Paso fault trends essentially east-west and merges with the Garlock fault near the east end of the El Paso Mountains. It appears to terminate west of the study area before reaching the Sierra Nevada (Dibblee, 1952) (Fig. 3). It crops out as a series of discontinuous traces, and its fault plane is vertical in the subsurface (Mabey, 1960). Although its outcrop pattern suggests that it is a strand of the Garlock fault, there is no evidence for left-lateral slip on the El Paso fault, and displacement of Quaternary alluvial fans along its trace shows that recent slip on the El Paso fault has been vertical and up on the north (Dibblee, 1952; Carter, 1980). The maximum throw on the fault exceeds 6 km.

Throughout most of its outcrop area, the Ricardo Group is tilted west-northwest toward the Sierra Nevada fault. The attitude of the tilted Dove Spring Formation is consistent with rotation accompanying fundamentally east-west extension between the north-trending Sierra Nevada fault and the east-northeast Garlock fault. The Sierra Nevada fault dips

~60° at the surface (Dibblee, 1967) but may flatten and underlie the Dove Spring Formation at depth. Early Miocene strata on the north slope of the El Paso Mountains dip generally 25°–30°. Dips decrease systematically upward to 5°–10° at the top of member 5 of the Dove Spring, above which exposures of member 6 appear essentially flat lying. The time of tilting is confined to late Miocene to Pleistocene by the overlying untilted Pleistocene sediments. Although the systematic upward and northwest-ward dip decrease could be suggestive of syndepositional basin growth, it could also reflect diminishing deformation due to increased distance from the El Paso Mountains uplift. Unconformities, which are typical of synsedimentary tilting, were not observed in the Dove Spring Formation, but there is abundant sedimentary evidence for diastemic exposure in the upper part of member 5.

The paleomagnetic data indicate that the Dove Spring strata have been rotated counterclockwise an average of 15° (Fig. 6). This rotation can be examined in more detail (Fig. 13) by viewing the magnetic data within separate time increments (D. W. Burbank and D. P. Whistler, unpub. data). We interpret these data to indicate that rotation of the Dove Spring strata was in part syndepositional. It appears to have commenced about 10 m.y. ago and to have proceeded systematically counterclockwise about 15°–20° between 10 and 7 Ma. Additional studies of the rotation both of isochronous ash beds within the Dove Spring and of the underlying Cudahy Camp strata are consistent with this interpretation (D. W. Burbank and D. P. Whistler, unpub. data). This rotation could possibly be related to counterclockwise rotations that are recorded at several localities in the central and western Mojave block to the south (Burke and others, 1982; Luyendyk and others, 1985; MacFadden and others, 1987), but which have poor temporal constraints (post-Paleogene to post–middle Miocene?). It appears much more likely that this Ricardo rotation is a direct response to sinistral shear along the nearby Garlock fault. As such, it suggests that movement along the Garlock fault commenced in this area at about 10 Ma.

Sequence of Deformation

Structural crosscutting relationships show that the El Paso basin has been affected by at least four episodes of structural deformation since the Goler Formation was deposited in the middle Paleocene: (1) northward tilting of the Goler Formation between late Paleocene and early Miocene time; (2) north-south extension and intrusion of east-west dikes in the early or middle Miocene, probably 15–17 Ma; (3) west-northwest tilting and related extension involving strata at least as young as 9 m.y. old; and (4) counterclockwise rotation beginning about 10 Ma. In addition, the basin was translated westward along the Garlock fault, probably penecontemporaneously with the 10- to 7-m.y.-old rotation. Changes in the orientation and style of structures of different ages are evidence that the basin was subjected to stresses which have varied significantly in orientation with time, including a switch from north-south to east-west extension between the early and late Miocene.

MIOCENE HISTORY OF THE EL PASO BASIN

Early and Early Middle Miocene

Deposition of the Cudahy Camp Formation began subsequent to northward tilting of the Goler Formation between the middle Paleocene and early Miocene. Tilting is most likely to have been caused by moderate uplift of the ancestral El Paso Mountains along an east-west trend. The basal conglomerate of the Cudahy Camp Formation was deposited over

the eroded basement complex and Goler Formation as a north-sloping bajada on the southern margin of the basin. Boulders as large as 1 m in diameter indicate that the source area was nearby. The conglomerates of the basal Cudahy Camp are dominated by clasts eroded from the intrabasinal pre-Miocene rocks now exposed in the El Paso Mountains, suggesting that an elevated, basement-cored area blocked transport of clasts from the Mojave volcanic province south of the Garlock fault.

Conglomerate deposition was followed by andesite and pyroclastic eruptions south and east of the present basin from 18 to 17 Ma. Subsequent basalt eruptions were accompanied by minor north-south extension in the basin, which produced east-west–trending dikes. Eruption of the Black Mountain Basalt between 17 and 15 Ma was the last major volcanic event in the El Paso basin.

The depositional basin of the Cudahy Camp need not have been deep to accommodate the preserved 300 m of sediments and volcanic rocks. The Cudahy Camp Formation accumulated with no evidence of basin growth through synsedimentary faulting or tilting. Stratigraphic relationships along the south margin of the El Paso basin suggest that the Cudahy Camp sediments and volcanics were restricted to the eastern portion of the El Paso basin, where the Paleocene Goler Formation is also preserved. Cudahy Camp rocks are absent from the western part of the basin, and the succeeding Dove Spring strata contain no evidence that a substantial volume of the Cudahy Camp strata was removed by late Miocene erosion. The depocenter of the El Paso basin may have thus been farther east in the early Miocene and may have shifted westward toward the Sierra Nevada fault during the late Miocene.

Middle and Late Miocene

The disconformity between the Cudahy Camp and Dove Spring formations spans the period from ~15–13.5 Ma. The lack of significant tilting between Cudahy Camp and Dove Spring strata suggests that movement on basin-controlling faults ceased following the event that caused tilting of the Goler Formation. The absence of clastic material derived from the Cudahy Camp and pre-Miocene rocks of the El Paso basin in Dove Spring conglomerates and sandstones indicates that older rocks did not constitute a significant sediment-source area.

Sediment accumulation resumed 13.5 m.y. ago with deposition of coarse alluvial fanglomerates in the lower part of the Dove Spring Formation. In contrast to the basal conglomerates of the Cudahy Camp Formation, clasts in the basal Dove Spring are almost entirely volcanic and of extra-basinal origin. Although these clasts cannot be linked with any specific source area, similar rocks are widely exposed in the western Mojave Desert. Sandstones in member 1 and lower member 2 of the Dove Spring reflect a predominantly basaltic or andesitic volcanic provenance consistent with that of the conglomerates. The reappearance in the basal Dove Spring of extra-basinal clasts up to 0.5 m in diameter and the change in source area can be cited as evidence of moderate uplift of the Mojave block in the middle Miocene, such that a sediment-transport network linking the Mojave block with the El Paso basin became established. Basal alluvial-fan deposits, such as the Cudahy Camp volcanics, are thickest in the central part of the basin, but by 13 Ma, the Dove Spring stream system spread westward toward the Sierra Nevada, and later Dove Spring deposits overstepped the El Paso Mountains basement complex on the southwest edge of the basin.

Middle to late Miocene drainage in the basin was to the north-northwest, transverse to basin-bounding tectonic elements. Volcanic-clast gravels from the Mojave block were deposited on alluvial fans near the south edge of the basin, and sand-sized sediment was transported toward the center of the basin by ephemeral braided streams. A persistent lake occupied the northern part of the basin for most of the late Miocene. Deposition of Dove Spring sediments was punctuated by pyroclastic and basaltic volcanic eruptions with vents probably located west of the basin.

A systematic upward increase in the ratio of quartz to lithic clasts in sandstones and conglomerates of the Dove Spring Formation was not accompanied by corresponding changes in paleocurrent directions. This suggests that progressive denudation of Tertiary volcanic cover led to exposure of basement rocks as erosion succeeded eruption in the Mojave block source area. Most Tertiary volcanism in the Mojave block occurred in the early to middle Miocene. Therefore, the accumulation of large volumes of new volcanic rocks in the source area had probably ended by Dove Spring time.
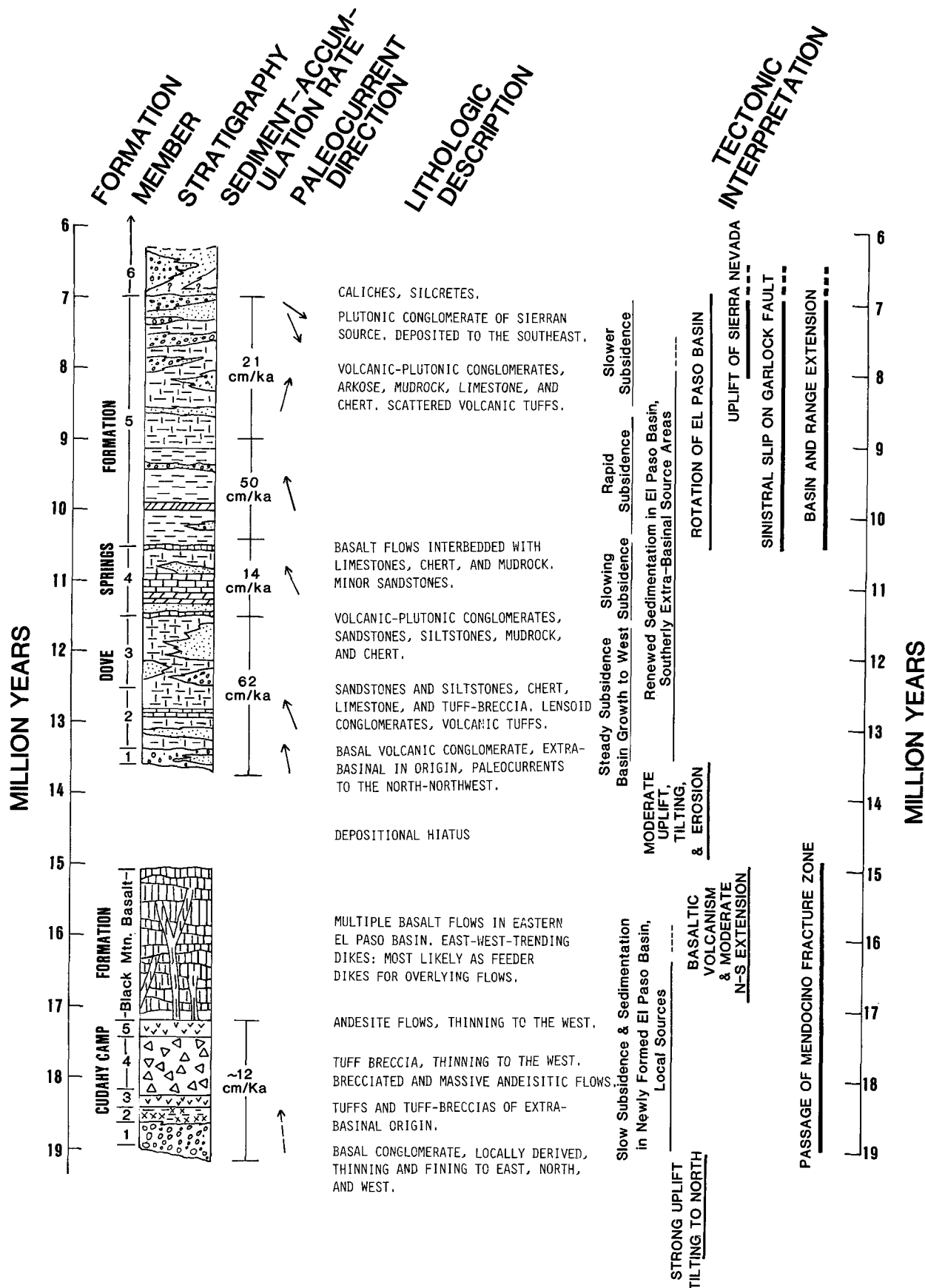
Beginning ~10 Ma, the El Paso basin began to be rotated counterclockwise, probably as a consequence of sinistral shear due to the initiation of left-slip motion along the Garlock fault near the southern margin of the basin. Such movement is also likely to signal the beginning of basin-and-range–style extension north of the fault. A sharp increase in apparent sediment-accumulation rates to 44 cm/ka (Fig. 8) accompanied the beginning of rotation between 10–9 Ma. This suggests relative uplift of the Mojave block source and increased subsidence rates in the basin, due to crustal thinning as extension began.

At about 8 Ma, a particularly significant compositional change occurred in the youngest sandstones and conglomerates of the Dove Spring (upper members 5 and 6). In the sandstones, a high proportion of quartz and alkali feldspars and an absence of lithic grains indicate a silicic plutonic source area. Granite and granodiorite boulders and gravel dominate the conglomerates. Although paleocurrent indicators are sparse in these sandstones, the Sierra Nevada can be identified as the source of this detritus with considerable confidence due to observable clast-size trends, facies relationships, and distinctive lithologies. The postulated morphotectonic emergence of the Sierra Nevada as a source for the ~8-m.y.-old upper Dove Spring sediments is consistent with estimates of accelerated uplift of the range between 10 and 3 Ma (Christiansen, 1966; Huber, 1981; Chase and Wallace, 1986). The apparent decrease in sediment-accumulation rates between 9 and 8 Ma (Fig. 8) is difficult to interpret in this context. It may be a response to tectonic disruption of the proximal basin margin due to precursor movements along the Sierra Nevada frontal fault, or it may result from the removal of some unknown quantity of member 5 during exposure and tilting associated with uplift of the Sierra Nevada. Following major uplift, rapid sedimentation could be anticipated adjacent to the frontal fault. Paleomagnetic data from restricted exposures in these proximal areas do suggest accelerated sedimentation. There are, however, insufficient data to determine reliable accumulation rates.

The dramatic change from extension in a north-south direction in the early Miocene to east-west extension in the late Miocene is evidence of the initiation of the system of basin-and-range faulting that has created present-day structures and topography north of the Garlock fault. The El Paso basin of Dove Spring time was considerably larger than the basin of the Cudahy Camp, and its western margin reached to the Sierra Nevada. This expansion of the basin may also have resulted from increased subsidence associated with the onset of basin-and-range extension.

DISCUSSION

The onset of the late Cenozoic extension which dominates the geology of the Basin and Range region is recorded in the late Miocene rocks of the Ricardo Group. Although this extension is intimately related to the function of the Garlock fault as a major left-slip discontinuity (Davis and

EL PASO BASIN

FORMATION MEMBER STRATIGRAPHY SEDIMENT-ACCUMULATION RATE PALEOCURRENT DIRECTION LITHOLOGIC DESCRIPTION TECTONIC INTERPRETATION

MILLION YEARS

21 cm/ka

CALICHES, SILCRETES.

PLUTONIC CONGLOMERATE OF SIERRAN SOURCE, DEPOSITED TO THE SOUTHEAST.

VOLCANIC-PLUTONIC CONGLOMERATES, ARKOSE, MUDROCK, LIMESTONE, AND CHERT. SCATTERED VOLCANIC TUFFS.

50 cm/ka

BASALT FLOWS INTERBEDDED WITH LIMESTONES, CHERT, AND MUDROCK. MINOR SANDSTONES.

14 cm/ka

VOLCANIC-PLUTONIC CONGLOMERATES, SANDSTONES, SILTSTONES, MUDROCK, AND CHERT.

62 cm/ka

SANDSTONES AND SILTSTONES, CHERT, LIMESTONE, AND TUFF-BRECCIA. LENSOID CONGLOMERATES, VOLCANIC TUFFS.

BASAL VOLCANIC CONGLOMERATE, EXTRA-BASINAL IN ORIGIN, PALEOCURRENTS TO THE NORTH-NORTHWEST.

DEPOSITIONAL HIATUS

MULTIPLE BASALT FLOWS IN EASTERN EL PASO BASIN. EAST-WEST-TRENDING DIKES; MOST LIKELY AS FEEDER DIKES FOR OVERLYING FLOWS.

ANDESITE FLOWS, THINNING TO THE WEST.

TUFF BRECCIA, THINNING TO THE WEST. BRECCIATED AND MASSIVE ANDEISITIC FLOWS.

TUFFS AND TUFF-BRECCIAS OF EXTRA-BASINAL ORIGIN.

BASAL CONGLOMERATE, LOCALLY DERIVED, THINNING AND FINING TO EAST, NORTH, AND WEST.

DOVE SPRINGS FORMATION

CUDAHY CAMP FORMATION — Black Mtn. Basalt

~12 cm/Ka

Slower Subsidence

Rapid Subsidence

Slowing Subsidence

Steady Subsidence Basin Growth to West Subsidence

Renewed Sedimentatiom in El Paso Basin, Southerly Extra-Basinal Source Areas

MODERATE UPLIFT, TILTING, & EROSION

Slow Subsidence & Sedimentation in Newly Formed El Paso Basin, Local Sources

ROTATION OF EL PASO BASIN

BASALTIC VOLCANISM & MODERATE N-S EXTENSION

STRONG UPLIFT TILTING TO NORTH

UPLIFT OF SIERRA NEVADA

SINISTRAL SLIP ON GARLOCK FAULT

BASIN AND RANGE EXTENSION

PASSAGE OF MENDOCINO FRACTURE ZONE

MILLION YEARS

Figure 14. Summary figure of the Miocene history of the El Paso basin. Chronologic control from magnetostratigraphic and radiometric studies is used to place sedimentologic and tectonic events in a precise temporal framework. The sediment-accumulation rates represent the mean, decompacted "instantaneous" rates for each interval. The vertical extent of lines associated with the tectonic interpretations is intended to indicate the time interval over which each event is interpreted to have occurred. Dashed lines indicate uncertainty concerning the precise initiation or termination of an event.

Burchfiel, 1973), it has, as previously noted, been postulated many times that a large down-to-the-north, dip-slip or strike-slip fault occupied the site of the present Garlock fault at some earlier time in the Cenozoic (Hewett, 1954; Nilsen and Clarke, 1975; Cox, 1982). The relatively thin (300 m), areally restricted, and locally derived deposits of the Cudahy Camp Formation, however, are suggestive of deposition in a small, restricted basin (Fig. 14), rather than in a regional, fault-controlled depression, such as that postulated for the Paleogene Garlock fault zone.

Although our interpretation of the Cudahy Camp Formation does not support the idea of an active, major pre-Garlock fault in the early Miocene, there are indications that tectonic stresses in the El Paso basin at this time would be at least consistent with dip-slip motion on an east-west fault south of the basin. East-west dikes cutting the Cudahy Camp and older rocks show that the El Paso basin was subjected to north-south tensional stresses sometime in the early to middle Miocene, but there is no evidence of net extension in that direction.

Plate-tectonic interactions between the North American plate and the Mendocino fracture zone may help to explain this early Miocene tectonic event. Several investigators (Blake and others, 1978; Dickinson and Snyder, 1979a; Glazner and Loomis, 1984) have noted that late Cenozoic events in many California sedimentary basins are associated in time with the progressive conversion of the western margin of North America from a subduction zone to a transform fault which accompanied northward passage of the Mendocino triple junction up the Pacific Coast (Atwater, 1970). Glazner and Loomis (1984) proposed a tectonic model which relates basin history to flexure of the North American plate over the subducted Mendocino fracture zone, modeled as a several-hundred-metre-high, east-west–trending, topographic step in the Farallon plate. Simulation of the North American plate's flexural properties shows that it would undergo north-south tension as it overrode the fracture zone in the Farallon plate (Glazner and Schubert, 1985). According to plate reconstructions, the Mendocino fracture zone would have passed through the latitude of the El Paso basin at about 17 Ma (Glazner and Loomis, 1984), that is, at the same time as eruption of the Black Mountain Basalt and probably at the same time that the east-west basalt dikes were emplaced in the Ricardo Group (Fig. 14). These events in the El Paso basin tend to support predictions (Glazner and Loomis, 1984; Glazner and Schubert, 1985) that north-south tension without net extension should be associated with passage of the Mendocino fracture zone. Consideration of the effects of the Mendocino fracture zone on the North American plate also predicts that tectonic uplift should follow the fracture zone's passage through a given area (Glazner and Loomis, 1984).

Data from the Ricardo Group also support this prediction. The middle Miocene hiatus between the Cudahy Camp and Dove Spring formations occurs shortly after the calculated time of the fracture zone's passage and is indicative of at least relative uplift above local base level (Fig. 14). Tectonic uplift, in the absolute sense, also occurred farther west in the San

Joaquin basin (Loomis and Glazner, 1986). This absolute uplift at the same time and latitude suggests that regional uplift did take place over a broad area after the Mendocino fracture zone passed through, and that the unconformity in the Ricardo Group is probably a result of this regional process.

The middle to late Miocene rocks of the El Paso basin, which overlie the unconformity, are distinctly different from the Cudahy Camp Formation and contain increasing evidence of the east-west extension which dominates the present geology of the region. The onset of east-west extension in southern California may also be related to the northward migration of the Mendocino triple-junction system. Theoretically, reorientation of lithospheric stresses south of the triple junction (Ingersoll, 1982) would produce a regional stress field conducive to east-west extension accommodated by north-south normal faults (Glazner and Bartley, 1984). Evidence from the El Paso basin indicates that basin-and-range–style extension began several million years after the apparent passage of the Mendocino fracture zone through the region. The sedimentary record of this extension during the Miocene is marked initially by renewed basin growth and rapid sedimentation north of the Garlock fault and culminates with accumulation in the El Paso basin of detritus from the newly emergent Sierra Nevada beginning about 8 Ma (Fig. 14).

Sedimentary evidence from the Dove Spring Formation does not directly mark the beginning of strike-slip movement on the Garlock fault, but because of the intimate relationship between the Garlock fault and extension east of the Sierra Nevada (Davis and Burchfiel, 1973), it seems that strike-slip displacement must have begun by the time the Sierra Nevada became manifest as a sediment-source area in the late Miocene. More precise specification of the time of inception of sinistral movement on the Garlock fault derives from the rotational data which point to strike-slip motion beginning ~10 Ma and from sediment-accumulation–rate data that indicate a coeval interval of rapid subsidence (Figs. 8 and 14), which we attribute to crustal thinning due to extension north of an active Garlock fault.

CONCLUSIONS

The Miocene volcanic and sedimentary rocks of the El Paso basin document the following tectonic events: (1) volcanism and north-south tension with no net extension, about 17–15 Ma in the early Miocene; (2) relative uplift about 15–13.5 Ma in the middle Miocene at the same time as absolute tectonic uplift farther west in the San Joaquin basin; (3) initiation of sinistral slip on the Garlock fault about 10 Ma; (4) the onset of east-west extension by at least 9 Ma; and (5) morphotectonic emergence of the Sierra Nevada by 8 Ma. These events can be related through plate-tectonic models to interactions between the North American, Pacific, and Farallon plates at the western margin of North America, and they provide some new age constraints for the uplift of the Sierra Nevada and for initial sinistral motion along the Garlock fault.

ACKNOWLEDGMENTS

assistance on this project. Special thanks are also due to the staff and residents of Red Rock Canyon State Park for their support and to Nancy Williams, Trileigh Stroh, and Miles Grant who helped with the field work.

REFERENCES CITED

Atwater, T., 1970, Implications of plate tectonics for the Cenozoic tectonic evolution of western North America: Geological Society of America Bulletin, v. 81, p. 3513–3536.

Baker, C. L., 1911, Notes on the later Cenozoic history of the Mohave Desert region in southeastern California: University of California Publications, Bulletin of the Department of Geology, v. 6, p. 333–383.

——— 1912, Physiography and structure of the western El Paso Range and the southern Sierra Nevada: University of California Publications, Bulletin of the Department of Geology, v. 7, p. 117–142.

Berggren, W. A., and van Couvering, J. A., 1974, The late Neogene: Biostratigraphy, geochronology, and paleoclimatology of the last 15 million years in marine and continental sequences: Developments in Paleontology and Stratigraphy, v. 2, 216 p.

Berggren, W. A., Kent, D. V., Flynn, J. J., and van Couvering, J. A., 1985, Cenozoic geochronology: Geological Society of America Bulletin, v. 96, p. 1407–1418.

Blake, M. C., Campbell, R. H., Dibblee, T. W., Jr., Howell, D. G., Nilsen, T. H., Normark, W. R., Vedder, J. C., and Silver, E. A., 1978, Neogene basin formation in relation to plate-tectonic evolution of San Andreas fault system, California: American Association of Petroleum Geologists Bulletin, v. 62, p. 344–372.

Burke, D. B., Hillhouse, J. W., McKee, E. H., Miller, S. T., and Morton, J. L., 1982, Cenozoic rocks in the Barstow Basin area of southern California—Stratigraphic relations, radiometric ages, and paleomagnetism: U.S. Geological Survey Bulletin 1529-E, 16 p.

Carter, B. A., 1980, Quaternary displacement on the Garlock fault, in Fife, D. L., and Brown, A. R., eds., Geology and mineral wealth of the California Desert; Dibblee volume: South Coast Geological Society, p. 457–466.

Chase, C. G., and Wallace, T. L., 1986, Uplift of the Sierra Nevada of California: Geology, v. 14, p. 730–733.

Christensen, M. N., 1966, Late Cenozoic crustal movements in the Sierra Nevada of California: Geological Society of America Bulletin, v. 77, p. 163–182.

Christiansen, R. L., 1961, Structure, metamorphism, and plutonism in the El Paso Mountains, Mojave Desert, California [Ph.D. dissert.]: Stanford, California, Stanford University, 180 p.

Clark, M. M., 1973, Map showing recently active breaks along the Garlock and associated faults, California: U.S. Geological Survey Map MI-741.

Cox, B. F., 1982, Stratigraphy, sedimentology, and structure of the Goler Formation (Paleocene), El Paso Mountains, California: Implications for Paleogene tectonism on the Garlock fault zone [Ph.D. dissert.]: Riverside, California, University of California, 248 p.

Cox, B. F., and Diggles, M. F., 1986, Geologic map of the El Paso Mountains Wilderness Study area: U.S. Geological Survey MF-1827, scale 1:24,000.

Cox, B. F., and Morton, J. L., 1980, Late Permian plutonism, El Paso Mountains, California: Geological Society of America Abstracts with Programs, v. 12, p. 103.

Davis, G. A., and Burchfiel, B. C., 1973, Garlock fault: An intracontinental transform structure, southern California: Geological Society of America Bulletin, v. 84, p. 1407–1422.

Dibblee, T. W., Jr., 1952, Geology of the Saltdale quadrangle, California: California Division of Mines and Geology Bulletin 160, 66 p.

——— 1967, Areal geology of the western Mojave Desert: U.S. Geological Survey Professional Paper 522, 153 p.

Dickinson, W. R., 1970, Interpreting detrital modes in graywacke and arkose: Journal of Sedimentary Petrology, v. 40, p. 695–707.

Dickinson, W. R., and Snyder, W. A., 1979, Geometry of triple junctions related to San Andreas transform: Journal of Geophysical Research, v. 84, p. 561–572.

Evernden, J. E., Savage, D. E., Curtis, G. H., and James, G. T., 1964, Potassium-argon dates and the Cenozoic mammalian chronology of North America: American Journal of Science, v. 262, p. 145–189.

Fisher, R. A., 1953, Dispersion on a sphere: Royal Society of London Proceedings, v. A 217, p. 195–305.

Gilbert, G. K., 1875, The geology of portions of Nevada, California, and Arizona: Report of the Geographical and Geological Survey West of the 100th Meridian, v. 3, p. 142–143.

Glazner, A. F., and Bartley, J. M., 1984, Timing and tectonic setting of Tertiary low-angle normal faulting in the southwestern United States: Tectonics, v. 3, p. 385–396.

Glazner, A. F., and Loomis, D. P., 1984, Effect of subduction of the Mendocino fracture zone on Tertiary sedimentation in southern California, in Nilsen, T. H., ed.: Sedimentary Geology, Special Issue, v. 38, p. 287–303.

Glazner, A. F., and Schubert, G., 1985, Flexure of the Nroth American lithosphere above the subducted Mendocino fracture zone and the formation of east-west faults in the Transverse Ranges: Journal of Geophysical Research, v. 90, p. 5405–5409.

Hamilton, W., and Meyers, W. B., 1966, Cenozoic tectonics of the western United States: Reviews of Geophysics, v. 4, p. 509–549.

Hewett, D. F., 1954, General geology of the Mojave Desert region, California: California Division of Mines and Geology Bulletin 170, p. 5–20.

Huber, N. K., 1981, Amount and timing of Late Cenozoic uplift and tilt of the central Sierra Nevada, California—Evidence from the upper San Joaquin River basin: U.S. Geological Survey Professional Paper 1197, 28 p.

Ingersoll, R. V., 1982, Triple-junction instability as cause for late Cenozoic extension and fragmentation in the western United States: Geology, v. 10, p. 621–624.

Johnson, N. M., and McGee, V. E., 1983, Magnetic polarity stratigraphy: Stochastic properties of data sampling problems, and evaluation of interpretations: Journal of Geophysical Research, v. 88, p. 1214–1221.

Johnson, N. M., Opdyke, N. D., Johnson, G. D., Lindsay, E. H., and Tahirkheli, R.A.K., 1982, Magnetic polarity stratigraphy and ages of Siwalik Group rocks of the Potwar Plateau, Pakistan: Palaeogeography, Palaeoclimatology, Palaeoecology, v. 37, p. 17–42.

LaViolette, J. W., Christenson, G. E., and Stepp, J. C., 1980, Quaternary displacement on the western Garlock fault, in Fife, D. L., and Brown, A. R., eds., Geology and mineral wealth of the California desert; Dibblee volume: South Coast Geological Society, p. 449–456.

Loomis, D. P., 1984, Miocene stratigraphic and tectonic evolution of the El Paso Basin, California [M.S. thesis]: Chapel Hill, North Carolina, University of North Carolina, 172 p.

Loomis, D. P., and Glazner, A. F., 1986, Middle Miocene tectonic uplift of the southern San Joaquin basin, California: American Association of Petroleum Geologists Bulletin, v. 70, p. 1003–1007.

Luyendyk, B. P., Kamerling, M. J., Terres, R. R., and Hornafius, J. S., 1985, Simple shear of southern California during Neogene time suggested by paleomagnetic declinations: Journal of Geophysical Research, v. 90, p. 454–466.

Mabey, D. R., 1960, Gravity survey of the western Mojave Desert, California: U.S. Geological Survey Professional Paper 316-D, 72 p.

MacFadden, B. J., Opdyke, N. D., and Woodburne, M. D., 1987, Paleomagnetism of the middle Miocene Barstow Formation, Mojave desert, southern California: Magnetic polarity and tectonic rotation: EOS (American Geophysical Union Transactions), v. 68, p. 291.

Merriam, J. C., 1913, New protohippine horses from Tertiary beds on the western border of the Mohave desert: University of California Publications, Bulletin of the Department of Geology, v. 7, p. 435–441.

——— 1919, Tertiary mammalian faunas of the Mohave Desert: University of California Publications, Bulletin of the Department of Geology, v. 11, p. 437–585.

Nakamura, K., Jacob, K. H., and Davies, J. N., 1977, Volcanoes as possible indicators of tectonic stress orientations: Aleutians and Alaska: Pure and Applied Geophysics, v. 115, p. 87–112.

Nilsen, T. H., and Clarke, S. H., 1975, Sedimentation and tectonics in the early Tertiary continental borderland of central California: U.S. Geological Survey Professional Paper 925, 64 p.

Palmer, A. R., 1983, The Decade of North American Geology 1983 geological time scale: Geology, v. 11, p. 503–504.

Samsel, H. S., 1962, Geology of the southeast quarter of the Cross Mountain quadrangle, Kern County, California: California Division of Mines and Geology Map Sheet 2.

Sclater, J. G., and Christie, P.A.F., 1980, Continental stretching: An explanation of the post-mid-Cretaceous subsidence of the central North Sea basin: Journal of Geophysical Research, v. 85, p. 3711–3739.

Smith, G. I., 1962, Large lateral displacement on the Garlock fault, California, as measured from offset dike swarm: American Association of Petroleum Geologists Bulletin, v. 46, p. 85–104.

Smith, G. I., and Ketner, K. B., 1970, Lateral displacement of the Garlock fault, southeastern California, suggested by offset of similar metasedimentary rocks: U.S. Geological Survey Professional Paper 700-D, p. D1–D9.

Whistler, D. P., 1969, Stratigraphy and small fossil vertebrates of the Ricardo Formation, Kern County, California [Ph.D. dissert.]: Berkeley, California, University of California, 269 p.